Review

The Importance of Rock Mass Damage in the Kinematics of Landslides

Davide Donati [1],*, Doug Stead [2] and Lisa Borgatti [1]

[1] Department of Civil, Chemical, Environmental, and Material Engineering, Alma Mater Studiorum—University of Bologna, 40136 Bologna, Italy
[2] Department of Earth Science, Simon Fraser University, Burnaby, BC V5A 1S6, Canada
* Correspondence: davide.donati17@unibo.it

Abstract: The stability and kinematics of rock slopes are widely considered to be functions of lithological, structural, and environmental features. Conversely, slope damage features are often overlooked and considered as byproducts of slope deformation. This paper analyzes and discusses the potential role of slope damage, its time-dependent nature, and its control on both the stability of rock slopes and their kinematics. The analysis of several major landslides and unstable slopes, combined with a literature survey, shows that slope damage can play an important role in controlling short- and long-term slope stability. Seasonal and continuously active events cause permanent deformation within the slope due to the accumulation of slope damage features, including rock mass dilation and intact rock fracturing. Rock mass quality, lithology, and scale control the characteristics and complexity of slope damage, as well as the failure mechanism. The authors propose that the role of slope damage in slope kinematics should always be considered in slope stability analysis, and that an integrated characterization–monitoring–numerical modelling approach can enhance our understanding of slope damage, its evolution, and the controlling factors. Finally, it is emphasized that there is currently a lack of guidelines or frameworks for the quantitative assessment and classification of slope damage, which requires a multidisciplinary approach combining rock mechanics, geomorphology, engineering geology, remote sensing, and geophysics.

Keywords: slope damage; slope kinematics; landslides; slope stability; rock slopes; rock mass quality; progressive failure; time-dependent mechanisms

1. Introduction

Landslides represent one of the most hazardous natural phenomena in mountainous regions, with significant social and economic impacts for the affected communities and infrastructures [1,2]. Landslides in rock are largely controlled by rock mass discontinuities, which affect their size and location at all scales, from outcrop-scale rockfalls to full-slope-scale rockslides. Discontinuities can have a sedimentological origin (e.g., bedding planes) or a structural origin (e.g., faults, joints, shear zones), and all can provide kinematic release to landslides [3,4].

The detachment and rapid displacement of landslides is often caused by single, specific events—often referred to as "triggers"—that generate a disturbance in the stress distribution within the slope, such as heavy rainfall events [5,6], earthquakes [7,8], and rapid slope submergence or drawdown of reservoirs [9,10]. Triggering events, often interpreted as the primary cause of slope failure, are generally characterized by relatively high energy; however, slopes affected by landslides may have often withstood stronger events in the past than those that resulted in failure. An example is described by Massey et al. [11], who investigated the effects of the 2010–2011 Canterbury earthquakes in New Zealand. They demonstrated that larger volumes of rock debris were mobilized—in the form of rockfalls and debris avalanches—during the 2011 (Mw = 6.2) Christchurch earthquake,

when compared to the 2010 (Mw = 7.1) Darfield earthquake, despite the greater intensity of the latter. Moreover, in several instances landslides have been found to have mobilized without any significant, high-energy event that could be recognized as the trigger. An example is the 9 May 1991 Randa rockslide (Switzerland, [12–14]), the detachment of which is considered to have been an event with no specific trigger. A similar observation was made for the 1965 Hope Slide [15,16], which detached during a cold spell in January without any obvious trigger [16]. The concept of "progressive failure" has often been used to explain such phenomena [17].

A progressive slope failure mechanism is driven by "progressive rock mass degradation" [17], which weakens the rock mass forming the slope through the formation and accumulation of damage [18]. The occurrence of earthquakes, heavy rainfall events, and other high-energy phenomena induces a progressive propagation of fractures and dilation of discontinuities within the rock mass, thereby decreasing the safety factor of the slope and predisposing the slope to failure during subsequent events [18].

Rock Mass and Slope Damage

The concept of damage in mechanics was introduced by Kachanov [19], who postulated that damage causes microstructural changes within a material, resulting in a decrease in strength. According to [19], the degree of damage (ω) in an isotropic body (e.g., a metal) can be described as the ratio between the damaged and undamaged area (A/A_0) in a finite section through the body. With regard to natural materials—specifically, rock masses—Paventi [20] considered damage as a reduction in quality or integrity, potentially leading to the eventual fragmentation or disintegration of the rock, and proposed a distinction between "inherent damage" and "mining-induced damage". Rock mass discontinuities, at various scales, that characterize the in situ rock mass (from microcracks, to joints and bedding, to regional faults or shear damage zones) are considered in [20] as inherent damage, whereas mining-induced damage occurs as a result of mining activity (e.g., blasting and/or mechanical excavation). Stead et al. [21], in discussing a modelling approach to simulate damage development, provided a more detailed classification of damage types, based on their origin, expanding on Paventi's [20] mining-focused perspective. Brideau et al. [22] provided a comprehensive discussion on the role of inherent damage and rock mass quality in the behavior and stability of rock slopes, discussing the relationship between tectonic damage and brittle fracture propagation (i.e., brittle damage).

Rock mass discontinuities at all scales—in addition to providing surfaces where landslides can displace, or from which blocks can detach—also decrease the strength of the rock mass constituting the slope [22]. To date, most works published in the literature focus on methods for characterizing the so-called inherent damage, along with its impacts on the detachment and displacement of landslides. However, the rock mass damage that is generated during and due to the deformation of the slope has seldom been addressed (e.g., [23]). In this work, the term "slope damage" is defined as the ensemble features that develop within or at the surface of a slope as a result of, or allowing for, the slope deformation. The rock mass dilation and fracturing that occur during earthquakes [18,24] or due to seasonal fluctuation of the water table [25], as well as fractures, scarps, and shear zones that form and propagate during the slope deformation [26,27], are all evidence of slope damage.

In general, inherent damage forms over a long timescale (i.e., geological timeframe), following lithification and exhumation of the material (e.g., bedding planes form during the deposition of the sediment that will ultimately constitute the rock and subsequent tectonics), whereas slope damage occurs in the short term after the formation of the slope itself (i.e., up to thousands of years, [28,29]). Hereafter, this paper refers to "rock mass damage" as a combination of inherent damage and slope damage (i.e., the total damage that a rock mass has experienced).

Generally, research on the topic of rock mass damage has combined characterization, monitoring, and modelling methodologies to investigate the development and evolution of slope damage and its effects on slope stability. Damage characterization entails the

observation, mapping, and description of damage features, typically performed using traditional field methods, geophysical approaches, or remote sensing techniques. Monitoring allows for the assessment of the spatial and temporal evolution of rock mass damage, and it can be conducted directly (i.e., by analyzing the progressive change and evolution of damage features) or indirectly (i.e., by investigating proxies for damage evolution, such as displacement or decay of seismic wave velocity). Modelling allows for the analysis of the factors that affect the formation, development, and accumulation of slope damage. Table 1 provides selected important literature published on slope damage research over the past two decades.

Table 1. Summary of relevant publications that describe the characterization, monitoring, and/or modelling of slope damage.

Activity	Summary of the Analysis	Reference
Characterization	Application of GPR for analysis of surface and internal damage in rock slopes	Toshioka et al. [30]
Characterization	Review of seismic-induced slope damage and landslides using historical data	Hancox et al. [31]
Modelling	Preliminary investigation of brittle damage and effects on progressive failure at the Randa rockslide site (Switzerland)	Eberhardt et al. [17]
Characterization, monitoring	Slope damage and displacement analysis of the Campo Vallemaggia landslide (Switzerland)	Bonzanigo et al. [32]
Characterization	Mapping of slope damage at the La Clapiére landslide (France) and effects on long-term evolution	Bedoui et al. [33]
Characterization	Investigation of the role of brittle and tectonic damage in slope and landslide kinematics	Brideau et al. [22]
Modelling	FDEM simulation of excavation-induced slope damage in large open pits and its effects on slope stability and evolution	Vyazmensky et al. [34]
Characterization	Assessment of damage at the Randa rockslide site (Switzerland) using geophysical methods	Moore et al. [35]
Monitoring	Application of the downhole acoustic emission technique to investigate slope damage accumulation in slopes	Cheon et al. [36]
Monitoring	Application of acoustic emission for the investigation of brittle damage accumulation due to frost cracking	Amitrano et al. [37]
Characterization, monitoring	Investigation of the effects of inherent and slope damage on slope stability through rock mass quality and displacement analysis	Agliardi et al. [38]
Modelling	Numerical simulation of slope damage development in biplanar and footwall failures	Havaej et al. [39]
Modelling	Numerical modelling of brittle slope damage at the Vajont Slide (Italy)	Havaej et al. [27]
Characterization	Identification, mapping, and interpretation of gravity-induced slope damage at the Vajont Slide (Italy)	Paronuzzi and Bolla [26]
Monitoring	Analysis of rockfall frequency (proxy for slope damage) through repeated laser scanner surveys	Kromer et al. [40]
Modelling	Analysis of the effects of groundwater pressure and slope damage development in open-pit mines	Vivas et al. [41]
Characterization	Assessment of the spatial distribution of co-seismic surface slope damage and landslides in historical earthquakes	Parker et al. [42]
Characterization	Mapping of open cracks in a rock slope using thermal imagery	Teza et al. [43]

Table 1. *Cont.*

Activity	Summary of the Analysis	Reference
Modelling	Analysis of the effects of spatial distribution of rock bridges in planar sliding failures in rock slopes	Bonilla-Sierra et al. [44]
Monitoring	Analysis of thermally induced deformation of an exfoliating rock slope using in situ and remote sensing methods	Collins and Stock [45]
Modelling	Simulation of hydromechanical fatigue and damage at the Campo Vallemaggia landslide (Switzerland)	Preisig et al. [25]
Modelling	Analysis of progressive failure driven by seismic damage and fatigue	Gischig et al. [18]
Modelling	Numerical analysis of long-term slope damage accumulation due to rock slope creep	Riva et al. [46]
Characterization	Automated mapping of brittle slope damage features at a retreating sea cliff	de Vilder et al. [47]
Characterization, modelling	Remote sensing mapping and numerical simulation of blast-induced damage in open-pit mine slopes	Lupogo [48]
Monitoring	Analysis of slope damage accumulation at Passo della Morte (Italy) using acoustic emission	Codeglia et al. [49]
Monitoring	Analysis of correlation between damage and creep deformation rates in open-pit mines	Danielson [50]
Modelling	Application of varied numerical methods to analyze slope damage development due to sub-level caving at the Kiruna mine (Sweden)	Hamdi et al. [51]
Modelling	Numerical analysis of long-term slope damage accumulation and progressive failure due to glacial retreat	Riva et al. [52]
Characterization	Identification of rock bridges along exfoliation joints through the analysis of thermal anomalies	Guerin et al. [53]
Modelling	FDM analysis of internal damage development at the Passo della Morte landslide (Italy)	Bolla and Paronuzzi [54]
Modelling	Simulation of brittle slope damage and its effects on the stability of the San Leo landslide (Italy)	Donati et al. [55]
Monitoring	Mapping of surface cracking at the 10-Mile Slide (Canada) using laser scanning	Donati et al. [29]
Modelling	Numerical simulation of slope damage at the Downie Slide (Canada), and correlation with inherent damage and basal surface morphology	Donati et al. [56]
Characterization, modelling	Analysis of inherent and slope damage at Hope Slide (Canada) and modelling of progressive failure due to damage along the incipient rupture surface	Donati et al. [16]
Characterization	Remote sensing analysis of inherent and slope damage at the Downie Slide (Canada)	Donati et al. [28]
Characterization, modelling	Investigation of slope damage induced by hydromechanical fatigue at the Checkerboard Creek landslide (Canada)	Piller [57]
Characterization	Brittle slope damage feature mapping within a rockslide scar	Paronuzzi and Bolla [58]
Characterization	Slope damage investigation at Civita di Bagnoregio (Italy) using remote sensing methods	Donati et al. [59]
Characterization, modelling	Analysis of the Marzellkamm rockslide (Austria) through rock mass mapping and numerical simulation	Rechberger and Zangerl [60]
Modelling	Application of the FDEM technique to investigate brittle damage development and accumulation	Sharif et al. [61]

2. Content, Structure, and Objectives

In this paper, the important role that slope damage plays in controlling the kinematic behavior of rock slopes and landslides—and, in turn, their stability and style of deformation—is discussed. Landslides previously described in the literature are analyzed with an emphasis on slope damage, investigating relationships between damage in varying lithology, rock mass quality, and at a range of slope scales. The importance of considering time as a factor in the formation and accumulation of slope damage is emphasized. The primary objectives of this paper are (1) to highlight factors that affect the types of slope damage features that develop within potentially unstable slopes; (2) to review potential approaches for the quantitative characterization of slope damage, highlighting their significance and existing challenges; and finally, (3) to demonstrate that the analysis of slope damage constitutes a critical step in the long-term stability analysis of rock slopes. The block diagram in Figure 1 outlines the structure of the paper and the topics covered in each section.
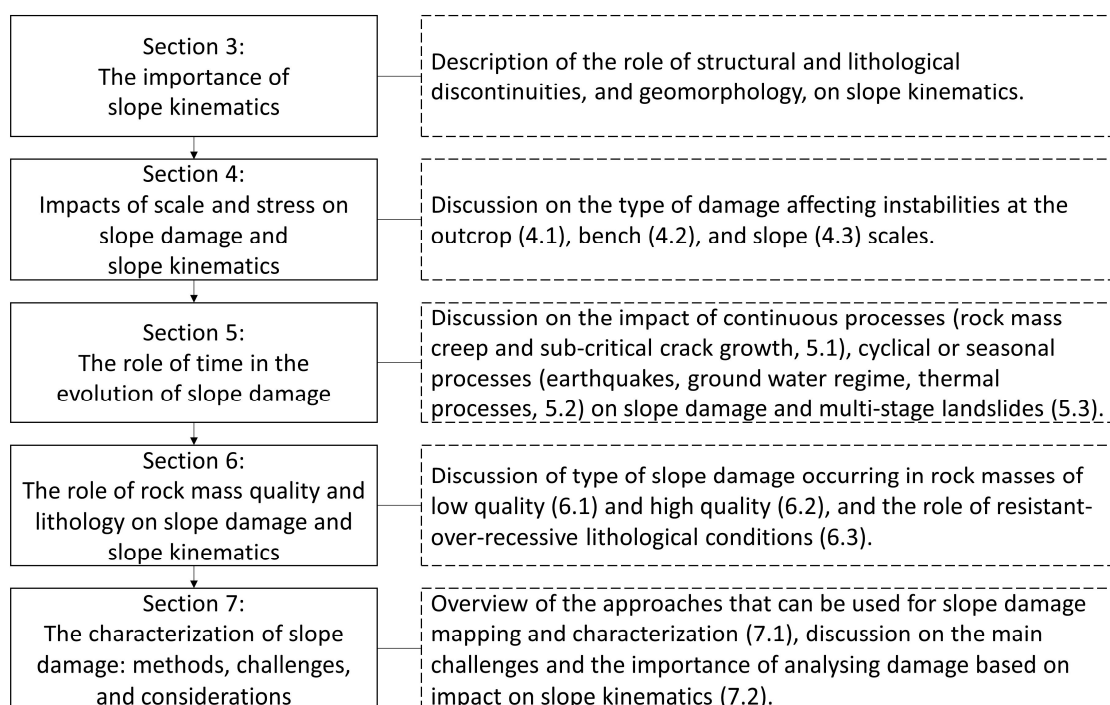
Section 3: The importance of slope kinematics	Description of the role of structural and lithological discontinuities, and geomorphology, on slope kinematics.
Section 4: Impacts of scale and stress on slope damage and slope kinematics	Discussion on the type of damage affecting instabilities at the outcrop (4.1), bench (4.2), and slope (4.3) scales.
Section 5: The role of time in the evolution of slope damage	Discussion on the impact of continuous processes (rock mass creep and sub-critical crack growth, 5.1), cyclical or seasonal processes (earthquakes, ground water regime, thermal processes, 5.2) on slope damage and multi-stage landslides (5.3).
Section 6: The role of rock mass quality and lithology on slope damage and slope kinematics	Discussion of type of slope damage occurring in rock masses of low quality (6.1) and high quality (6.2), and the role of resistant-over-recessive lithological conditions (6.3).
Section 7: The characterization of slope damage: methods, challenges, and considerations	Overview of the approaches that can be used for slope damage mapping and characterization (7.1), discussion on the main challenges and the importance of analysing damage based on impact on slope kinematics (7.2).

Figure 1. Flowchart illustrating the important aspects of slope damage presented in this paper.

3. The Importance of Slope Kinematics

The combined effects of discontinuities and slope morphology define the kinematic configuration of the slope, hereafter referred to as slope kinematics. Slope kinematics controls the style of deformation and displacement, along with the potential failure mechanism of the slope.

The presence of a daylighting, basal release surface is generally a critical requirement for the displacement of planar landslides [62]. However, the availability and critical importance of lateral release surfaces—provided, for instance, by tectonic structures or bedding planes—is often ignored with the assumption of plane strain conditions and the use of often inappropriate 2D slope stability analyses [63]. The absence of such release features in a slope effectively prevents a landslide or block from achieving a condition of "kinematic freedom", which can be defined as the capability of a discrete, removable (e.g., physically separated by discontinuities) volume in a rock slope to displace due to gravitational force. Similar considerations can be made for toppling failures, which require lateral release surfaces for the columns to topple out of the slope. Conversely, tetrahedral wedge failures are characterized by a block sliding along two intersecting discontinuities

that simultaneously constitute both lateral and basal release surfaces. In this case, the plunge and trend of the line of intersection control the kinematic freedom of the block, based on whether the intersection daylights or not (i.e., the line of intersection plunges out of, and with a lower angle than, the slope) [62]. While these basic failure mechanisms (e.g., planar sliding, wedge sliding, toppling) can occur at all scales, the characteristics of the release surfaces can differ. At the outcrop/bench scale, the detachment of kinematically free blocks occurs along single discontinuities (e.g., joints). At progressively larger scales (e.g., mountain slope/multi-bench pit scale), release surfaces can be constituted by multiple discontinuities, sometimes combined to define stepped or irregular surfaces (e.g., [64]).

In evaluating slope kinematics, consideration should be given to the morphology of the slope. In research on translational and toppling failure mechanisms, Brideau and Stead [3,65] used 3D distinct element numerical modelling to simulate instabilities in slopes with varying discontinuity orientation and slope morphology (i.e., slope angle and strike). They noted that the behavior and evolution of the instability, in terms of the involved volumes and displacement direction, is strongly related not only to the angles of intersection between discontinuities and between discontinuities and the slope, but also to the lateral confinement of the slope. The lack of lateral support within a slope (e.g., due to the presence of deeply incised gullies or a significant change in slope orientation) is more effective than lateral release surfaces (e.g., tectonic surfaces, such as joints or faults) in allowing slope deformation and failure [3,65]. In other words, slope morphology is a primary factor of control over the kinematic freedom of a landslide, beyond the simple influence of daylighting of basal release surfaces. The spacing of discontinuities also plays a role in controlling the size of the blocks that characterize the rock mass which, in turn, can potentially affect both slope kinematics and stability. Corkum and Martin [66] and Wolter et al. [67] investigated the impacts of block number and block size on the behavior and evolution of the slope at Block 731 (at the abutment of the Revelstoke Dam, in Canada) and the Vajont Slide (Italy), respectively.

Depending on environmental conditions and geomorphological processes, the morphology of rock slopes can change over relatively short times. In alpine areas, the erosive action of glaciers causes steepening in the lower slopes and successively promotes instability by reducing slope support as the glacial ice thins and retreats from the valley [68–70]. Although the buttressing action of glaciers (i.e., due the weight of the ice) is debated [71,72], the effect of glacier retreat on slope kinematics is widely recognized; many large rock slope instabilities initiated as the retreat of the glacier body caused a decrease in support for the slope—particularly in the lower part, where stresses concentrate due to increased steepness [28,68]. Fluvial erosion produces similar effects [73,74], the difference to glacial erosion being that the erosive action occurs with no or limited lateral support for the slope (i.e., due to the formation of fluvial terraces) [75]. The combined effect of wave motion and chemical alteration (e.g., due to dissolution) can also result in the failure, steepening, and retrogression of coastal cliffs [76,77].

In the shorter term, human environmental activity can also produce effects on slope kinematics similar to those of glacial and fluvial erosion. The excavation and steepening of rock slopes are common activities for the construction of linear infrastructure such as roads, railroads, and power lines in mountainous regions. Recently, such activities have been associated with an enhanced susceptibility to slope failure due to changes in stress concentrations and daylighting of geological structures (acting as basal release surfaces), as a result of the increased slope angle [78,79]. Open-pit mining activity, entailing the steepening and/or creation of new slopes, also has the potential to generate slope instabilities at various scales [80,81].

Undermining can also occur through both natural and anthropogenic actions, impacting slope kinematics, particularly where overhanging, vertical, or sub-vertical slopes exist, allowing blocks of varying sizes to detach and displace in freefall as a result of a lack of basal support [47]. This process, however, is necessarily accompanied by a certain amount of damage development, required to break any intact rock bonds (i.e., rock bridges, see

par. 3.3) that can allow the rock volume to remain in place for a certain time (ranging from minutes to hundreds of years) on sub-vertical slopes [45,82]. Slope damage is often a critical factor in not only controlling, but also changing the original slope kinematics. The deformation of slopes and displacement of landslides may occur through kinematic mechanisms that were not feasible when considering the orientation, persistence, and spacing of rock mass discontinuities alone, with the effect of the slope damage evolution being to create increased kinematic freedom. The mechanisms and processes through which slope damage can control landslide and rock slope behavior are described in the following sections.

4. Impacts of Scale and Stress on Slope Damage and Slope Kinematics

The type and characteristics of slope damage—in terms of spatial distribution and intensity—that develop within a slope are strongly controlled by the scale of the slope and its instability. According to [80], the scale of the slope instability can be qualitatively distinguished as outcrop scale, bench scale, and multi-bench (or slope) scale. Outcrop scale typically entails instabilities that develop in natural or engineered slopes, which can be characterized by an elevation up to 4–6 m, with relatively low stress magnitudes. Bench scale entails instabilities in slopes with a height comparable to that of open-pit benches—up to 20–30 m—characterized by an increased (but still low) stress magnitude. Multi-bench or slope scale comprises slope instabilities that involve large areas and volumes of rock mass and are generally characterized by rupture surfaces located at depths within the slope, along with higher stress magnitudes across the landslide body. It is important to note that the size of the slope (e.g., the vertical height) per se is not a direct indication of the type or size of instability (and, in turn, the type of slope damage) that can develop. For instance, the detachment of small blocks (e.g., a rockfall) from a high, vertical rock slope will still involve damage processes that are typically observed for outcrop-scale instabilities. In the following sections, an overview of the type and spatial distribution of slope damage features—as a function of the scale of the instability—and their effects on slope kinematics is provided.

4.1. Slope Damage at the Outcrop Scale

At the outcrop scale, instabilities in a rock mass generally involve the mobilization and detachment of discrete blocks bounded by planar discontinuities. The relative orientation and spacing of discontinuities define the shape and size of the blocks (see [83]), which can displace and fail through simple kinematic mechanisms such as planar sliding, wedge sliding, and block toppling. In general, low stress magnitudes (up to 100–150 MPa, considering a 25 KN/m^3 unit weight and a 4–6 m slope) occur along the discontinuities bounding the block, largely as a function of the orientation of the discontinuities and the unit weight of the rock mass. When such discontinuities are "fully persistent"—which means that no in-plane or out-of-plane rock bridges (see [82]) occur along the discontinuity surface—then the block can displace with limited development of damage, including shearing of asperities along the discontinuity surface (Figure 2a) (e.g., [84]). Conversely, the presence of even a limited amount of rock bridges along the release surface can effectively stabilize the block (Figure 2b). As a result, slope damage, in the form of brittle failure of the rock bridge, must occur for the failure to progress [82] (Figure 2c). In this sense, slope damage can be required in order to allow blocks to detach, whereas the kinematics (i.e., the failure mechanism) of the single block is not generally affected. According to the block theory, however, the stability and detachment of a single block (referred to as a "key block", [85,86]) can induce the propagation of the instability to blocks that were previously stable, potentially modifying the stability of slopes at the outcrop scale and beyond.
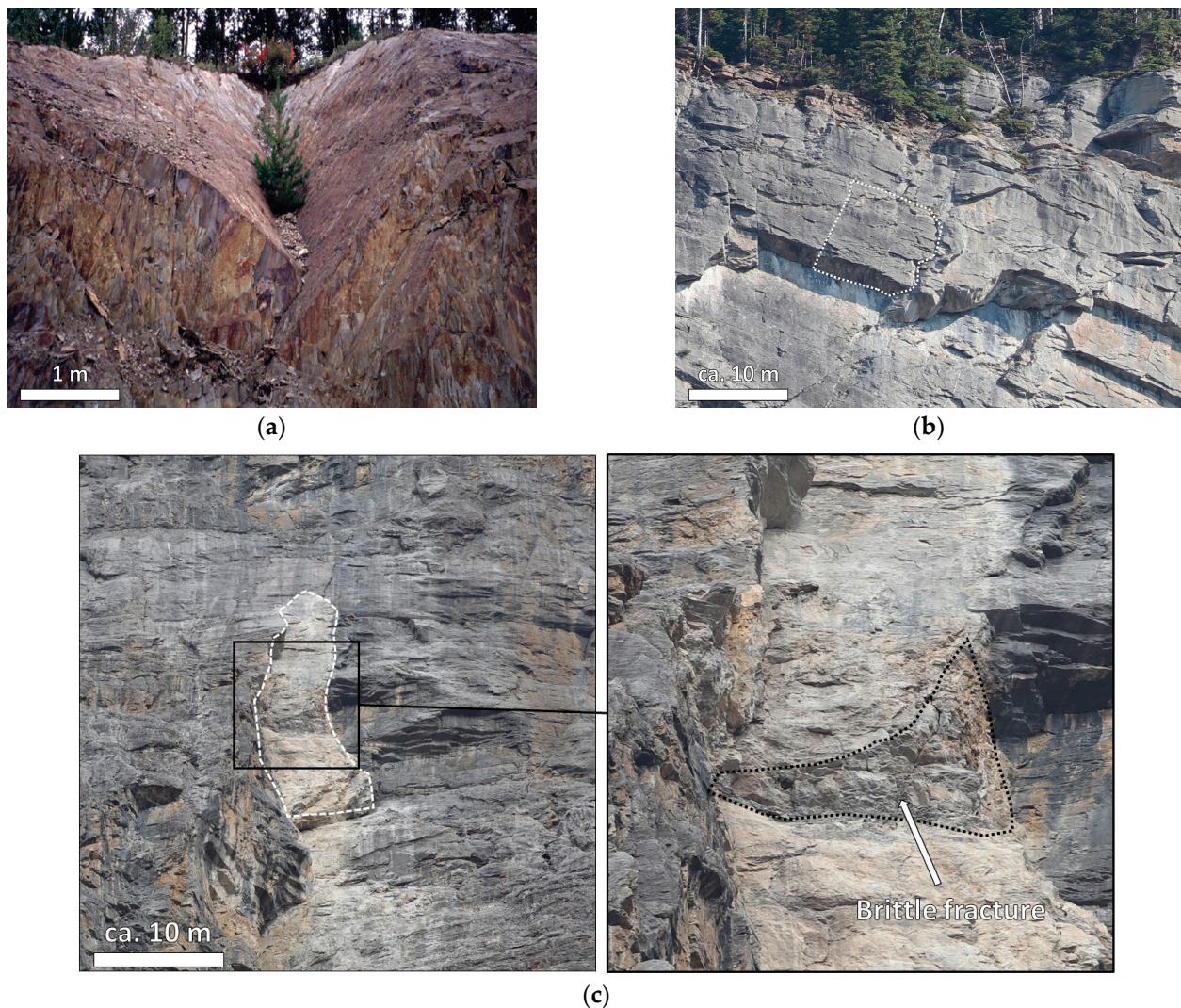
Figure 2. Outcrop-scale instabilities and associated slope damage features: (**a**) Release surface of a structurally controlled wedge along a roadcut near Jasper (Alberta, Canada). No significant indication of rock bridge failure is visible, suggesting that the detachment occurred during or shortly after the excavation (i.e., due to reduction in support and confinement), possibly in addition to the shearing of asperities along the discontinuity surfaces. (**b**) An incipient rockfall at Takakkaw Falls in Yoho National Park (British Columbia, Canada) is outlined by the white, dotted line. The overhanging block is held in place by rock bridges along the release surfaces. Their location and size are unknown. Progressive detachment of surrounding blocks may result in a reduction in lateral confinement and stress concentration, potentially inducing a cantilevering effect and subsequent rock bridge failure. (**c**) Fresh rockfall scar at the Weeping Wall, along the Icefield Parkway (Alberta, Canada). A rough surface indicating a failed out-of-plane stepped rock bridge surface (brittle slope damage feature) is outlined by the dotted black curve.

The gradual detachment of rockfalls from vertical or sub-vertical rock slopes is often controlled by progressive undercutting and a decrease in the lateral support of blocks, which also result in the stepped appearance of the slope surface (e.g., Figure 2b). Depending on slope morphology, slope and joint angle, structure, and rock bridge distribution, the detachment of rockfalls can be the result of (a) gravity-controlled tensile failure of rock bridges, with subsequent detachment and freefall of blocks; (b) failure due to concentration of tensile stresses within rock bridges along the side of overhanging blocks, which can be conceptualized as cantilevering beams; or (c) translation shear-dominated failure of in-plane rock bridges along the sides of overhanging blocks.

4.2. Slope Damage at the Bench Scale

At the bench scale, the mobilization of landslides remains largely controlled by discontinuities that result in structurally controlled failures. From a kinematic perspective, such failures do not generally require internal deformation of the block, and the potential failure mechanisms observed are similar to the outcrop scale (e.g., planar sliding, wedge sliding, toppling). However, the increased size of the instability may entail the occurrence of more complex release surface morphologies, comprising multiple, interconnected discontinuities forming stepped surfaces [87,88]. Such an increase in rupture surface complexity can be observed at several landslide sites, including the Hope Slide (characterized by a stepped basal surface, [89]) and the Frank Slide (which displaced along a complex rupture surface comprising structural discontinuities including bedding planes, joints, and a low-angle thrust fault [90]).

As the volumes involved in the slope instability increase, higher stresses will occur along the release surfaces, promoting failure of intact in-plane and out-of-plane rock bridges. The failure of rock bridges occurs predominantly in tension, particularly in the case of out-of-plane rock bridges. However, for higher dip angles of the basal release surface (i.e., in planar sliding) or line of intersection (i.e., in wedge instabilities), the shear stress increases, promoting failure of in-plane rock bridges [44,82]. Conversely, an increase in stress magnitude normal to the basal release surface will promote shearing of asperities, resulting in a reduction in the friction angle towards residual values [91].

From a kinematic perspective, tensile and shear damage that results in the failure of rock bridges along otherwise fully persistent release surfaces does not significantly impact the overall kinematics of the slope. However, localized damage accumulation can allow for the failure of blocks that are seemingly irremovable due to the lack of a daylighting release surface (for planar sliding)—as in the case of footwall failures [39]—or line of intersection (for wedge sliding), as in the case of non-daylighting wedges [92]. In these cases, the accumulation of slope damage results in the formation of a new release surface, effectively modifying the kinematics of the slope and allowing the failure to occur.

4.3. Slope Damage at the Multi-Bench Scale

Multi-bench instabilities commonly involve large volumes of rock masses and extend over large areas of the rock slope. Slope-scale instabilities can vary, including (a) fully structurally controlled instabilities, in which the landslide detaches and displaces along geological structures or lithological features without the need for any significant internal deformation for the failure to occur, and (b) slope-damage-controlled landslides, in which the failure becomes kinematically possible only after a certain amount of internal deformation. The 1987 Val Pola landslide (Italy, [93,94]) is an example of a fully structurally controlled slope-scale failure (Figure 3a). This event involved the displacement and failure of a 40 million m^3 wedge-shaped landslide in rock, the rupture surface of which was a combination of faults and schistosity planes. Conversely, slope-scale instabilities such as the Vajont Slide (e.g., [26,27,95], Figure 3b) and the Downie Slide (e.g., [28,96])—characterized by a bi- or multiplanar basal surface—require internal deformation within the transition zone—a prism-shaped volume of rock mass at the interface between the active block (constituting the upper part of the landslide, where the basal surface has a higher dip angle) and the passive block (the lower part of the landslide, with a lower basal surface dip angle). Within such a transition zone, sometimes referred to as "Prandtl prism" [97], high compressive and shear stresses occur, allowing slope damage to develop as a complex combination of rock mass discontinuity dilation, intact rock failure, fracture propagation, and shearing of asperities along discontinuity planes.
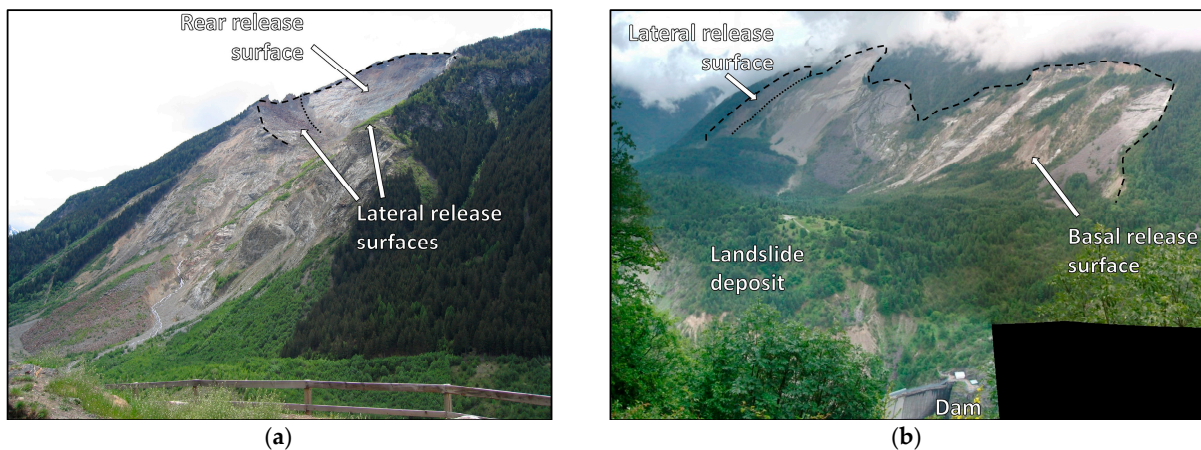
(a)   **(b)**

Figure 3. (**a**) Photograph of the Val Pola landslide from the valley (public domain). Note the rear and lateral release surfaces that formed a wedge-shaped landslide body. The maximum width of the headscarp is approximately 750 m. (**b**) Photograph of the Vajont Slide from the opposite valley slope. The outcropping bedrock scar forms the high-angle part of the basal release surface. The low-angle part is covered by the deposit. The Col Tramontin Fault forms the lateral release surface (left-hand side of the panorama). In the foreground, the Vajont Dam is visible. The width of the scar is approximately 2000 m.

5. The Role of Time in the Evolution of Slope Damage

The formation and accumulation of slope damage is often a process that develops over time, at rates that depend on the scale, stress, and mechanism of slope damage. The mechanisms responsible for the development of time-dependent slope damage can be distinguished (see [98]) between (a) continuously active processes, such as creep and subcritical crack growth, which are largely driven by gravity; and (b) episodic or cyclic processes, generally driven by natural phenomena such as earthquakes, extreme rainfall events, seasonal groundwater fluctuations, and temperature cycles, which weaken the slope through fatigue-related mechanisms (Figure 4).
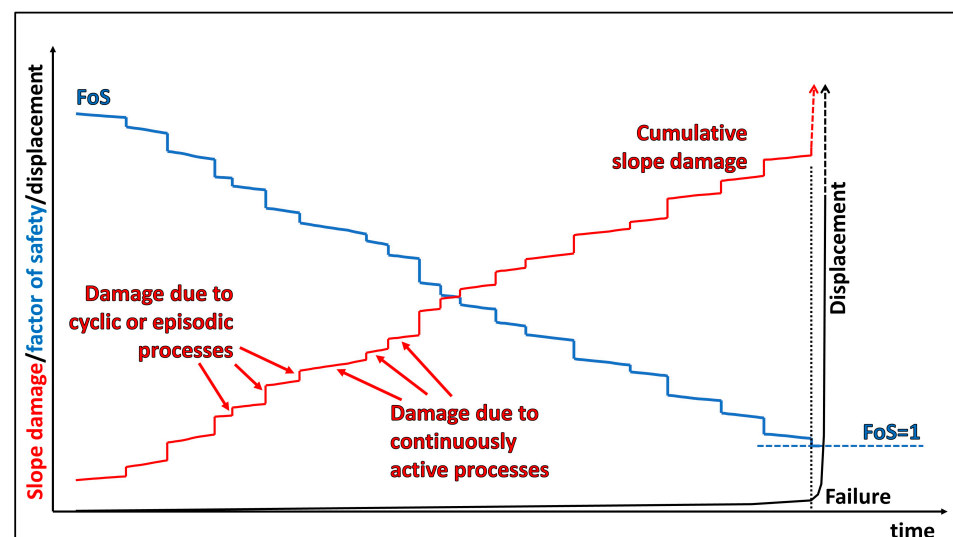
Figure 4. Conceptual representation of the correlation between cumulative slope damage, factor of safety (FoS), and displacement. Note that the relative importance (i.e., the rate and magnitude of displacement) of cyclic or episodic and continuously active processes is conceptual only, and it strongly depends on the location of the site, as well as the geological, geomorphic, and environmental conditions.

5.1. Effects of Continuously Active Processes

The term "creep" is used to describe slow deformation that occurs without significant changes in stress conditions. The first studies on material creep largely involved analysis of isotropic materials [99,100], the deformation of which was found to follow a four-stage time–deformation curve [101]. In fractured rock masses, this process—referred to as "mass rock creep" (MRC, [102])—is responsible for the deformation of rock slopes without a discrete rupture surface, and it can occur both in natural rock slopes ([102]) as well as in engineered rock slopes [50]. The basal surface of large, deep-seated landslides can also comprise a transition zone, where significant creeping, time-dependent slope damage occurs within a shear zone (e.g., [28,32]). The deformation of creeping rock slopes is accompanied, particularly in heavily foliated lithologies, by the development of gravity-induced folds and kink bands that can correlate with foliation bands along which the creeping rock mass locally displaces [102]. The "ductile" deformation that contributes to the creation of fold and kink bands is associated with a decrease in rock mass quality (e.g., increased degree of fracturing) that can play an important role in reducing the slope's stability (e.g., [38]). In his review on MRC mechanisms, Chigira [102] showed various examples of landslides where part of the release surface was created by the folding and subsequent shearing of the rock mass at the base of a creeping slope. In this situation, MRC can significantly impact slope kinematics by causing the formation of a previously unavailable release surface.

In brittle rock, creep deformation is often accompanied by subcritical crack growth. Fracture mechanics studies show that, once a load is applied, stress concentrations occur at the tip of fractures in intact rock [103]; as the applied load increases, the fracture becomes more likely to propagate rapidly in an uncontrolled manner. Subcritical crack growth is a process by which the brittle propagation of fractures occurs relatively slowly at lower stress magnitudes [104,105]. The effects of subcritical crack growth (in shear) on slopes have been conceptually investigated, using numerical modelling, by Kemeny [106,107]. Later applications include the investigation of time-dependent tensile failure of in-plane rock bridges [108]. Donati et al. [16] proposed that subcritical crack growth was a critical factor in the progressive failure of the 1965 Hope Slide, based on geomorphic and numerical modelling analyses (Figure 5). In particular, they suggested that the post-glacial detachment of a landslide from the same slope caused a stress concentration along the incipient rupture surface. Such a stress concentration promoted long-term fracture propagation that ultimately caused the catastrophic failure in January 1965. The interpretation of the landslide as a result of a long-term creeping slope deformation was previously proposed by [109]. The potential role of time-dependent creep along rupture surfaces was also investigated by Grøneng et al. [110], who employed a numerical modelling approach to investigate the Åknes Slide (Norway). By using varying sets of mechanical parameters for the material forming the basal shear zone, they simulated the long-term displacement and behavior of the landslide as a result of the progressive accumulation of slope damage. The progressive geomorphic evolution of the slope (e.g., due to glacial or fluvial erosion) may also induce a permanent stress redistribution within the slope, representing a potential cause for the initiation of creep deformation [111].
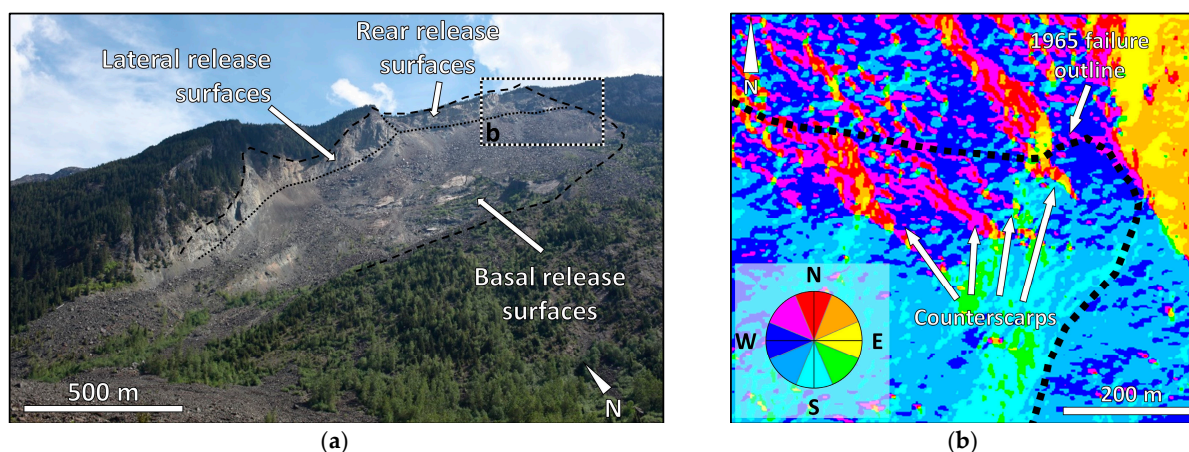
Figure 5. (**a**) View of the Hope Slide from the deposit. The lateral, rear, and basal release surfaces are outlined. The black-and-white dotted polygon outlines the approximate boundaries of the map shown in b. (**b**) Pre-failure aspect map of the headscarp area, derived from a structure-from-motion 3D model created using historical air photos. A series of counterscarps is highlighted that have been interpreted as the result of a long-term slope deformation, initiated with a post-glacial slope failure, driven by creep and subcritical crack growth along the incipient basal surface.

5.2. Effects of Episodic or Cyclic Processes

As opposed to creep and subcritical crack growth, changes in stress concentrations caused by episodic and cyclical processes may induce instantaneous slope deformations that are only partially recovered at the end of the process. The unrecovered fraction of slope deformation results from the formation and accumulation of slope damage during the event [18]. The rate at which slope damage induced by natural processes accumulates depends on the frequency and intensity of such processes. High-magnitude earthquakes are generally responsible for significant seismic-induced slope damage [18]. Limited work in the published literature has been undertaken to define a minimum earthquake Mw (moment magnitude) threshold above which seismic-induced slope damage (e.g., co-seismic fracturing) occurs and becomes evident at the slope surface. However, Marc et al. [112], in their review, suggest that in most cases co-seismic landslides occur for earthquakes greater than Mw = 5. A similar result was also drawn for co-seismic landslides that occurred in large open pits [113]. Thus, such a threshold can be considered as the lower limit for the development of seismic-induced slope damage. However, the strength of the rock mass forming the slope may play an important role, and the development of co-seismic damage in slopes constituted by weak rock masses should also be considered. Co-seismic slope damage features largely consist of surface and internal cracks, which can result from the combination of (a) opening of pre-existing tectonic discontinuities and rock mass dilation, and (b) formation of new fractures and brittle propagation of discontinuities [24,72,114]. Co-seismic cracking and rock mass dilation caused by subsequent earthquakes progressively accumulate and propagate at depth from the surface. Damaged and fractured rock masses are characterized by lower seismic wave velocities than undamaged rock masses. In fact, slope damage was found to enhance seismic amplification even more effectively than material contrasts and topographic factors [115]. Thus, the initiation of slope damage in rock slopes located in seismic areas induces a feedback process that makes damaged slopes even more prone to the future development of seismic damage, weakening the slope and promoting failures during subsequent earthquakes [11,115].

Seasonal groundwater fluctuations and, by extension, extreme rainfall events [18] also impact slope damage accumulation and, in turn, the long-term stability of rock slopes. Field monitoring and numerical modelling analyses conducted at the Campo Vallemaggia landslide (Switzerland) indicated that high, artesian groundwater pressures control both the displacement of this slow, deep-seated landslide, as well as the progressive accumulation

of slope damage within the landslide body, through a mechanism of hydromechanical fatigue [25,32,116].

Temperature cycles are also known factors in the development of slope damage. The most significant impact occurs in high-elevation and high-latitude regions where the brittle propagation of fractures may occur due to (a) freeze/thaw cycles, which cause water within open joints to continuously freeze and melt, forcing the opening of fractures due to volume-induced ice-jacking [117,118]; and (b) segregation ice growth, which entails a migration of unfrozen pore water, driven by a temperature gradient, towards freezing sites where ice lenses grow, causing stress accumulation at fracture tips [119,120]. Fracture opening and propagation was found to be a critical process in controlling the detachment of rockfalls in high mountain areas [121] and, in some cases, also the retreat of sea cliffs [122]. A direct correlation was observed between the amount of slope damage accumulated through freeze/thaw cycles and the quality and degree of fracturing of rock masses [123]. From a kinematic perspective, fracture propagation due to freeze/thaw cycles or segregation ice growth can promote outcrop-scale instabilities, notably by allowing the formation of fully persistent rupture surfaces for rockfalls. Indeed, the impact of these mechanisms (i.e., the capability of the process to cause fracture propagation) is limited to the surface of the rock slope, reaching depths of up to a few meters, depending on the thermal conductivity of the rock mass [121]. Conversely, the size of the blocks that can potentially detach largely depends on the discontinuity persistence and spacing [121].

Thermal expansion and contraction of rock masses due to changes in temperature is also a known factor that can impact the stability of rock slopes by causing discontinuity and rock mass dilation, as well as fracture propagation. Gunzberger et al. [124] investigated a 2000 m^3 rockfall that detached in 2007 from the Rochers de Valabres rock slope (France). Noting the absence of any potential trigger (e.g., rainfall, earthquake), they used field monitoring methods and numerical modelling to highlight the impact of temperature cycles on permanent joint deformation, which was recognized as a contributing factor to the rockfall detachment. A similar approach was also used to investigate the impacts of temperature cycles on the stability of the present-day Randa rock slope (i.e., after the 1991 failures). In their work, Gischig et al. [125] used numerical modelling to investigate the distribution of opening and propagating discontinuities, noting a good correlation between the displacement simulated in the model and that observed from the monitoring system (including surface and in-hole extensometers). The potential role of thermal cycles in the detachment of rockfalls, due to progressive degradation of rock bridges along exfoliation joints, was investigated by Collins et al. [45].

5.3. Time-Dependent Processes and Multistage Landslides

Time-dependent processes are sometimes initiated by sudden changes in slope morphology—notably, slope failures that promote retrogression or lateral propagation. Multistage failures are commonly controlled by slope damage that accumulates within the rock mass (e.g., along an incipient or developing rupture surface) after the occurrence of an initial major event, particularly where the volume involved represents a key block [86]. The 2019 Joffre Peak landslide is an example of such a process (Figure 6a), involving the detachment of two landslides, nearing a total of 6 million m^3, from the northern slope of Joffre Peak (BC, Canada, [126]). The first landslide detached on 13 May 2019 and was interpreted as the result of permafrost degradation that increased water pressure (thereby decreasing the effective stresses) along the rupture surface [126]. The second landslide detached on 16 May 2019 and involved a structurally controlled volume of rock mass displacing into the empty void left by the first landslide. Both failures were seemingly promoted by a certain amount of slope damage that accumulated along the release surfaces prior to the failures. Fracture propagation along the basal release surface (formed by low-persistence discontinuities separated by in-plane and out-of-plane rock bridges) played a role in providing kinematic freedom to the first landslide [127]. The subsequent decrease in lateral support promoted slope damage accumulation along the basal release surface of the second

block, which ultimately failed three days later. In view of the geomorphic and regional configuration of the area, a combination of subcritical crack growth (also promoted by increased water pressure), co-seismic slope damage, and uncontrolled fracture propagation after the first landslide may have contributed to the slope failures. The Palliser rockslide (AB, Canada) is another example of a multistage landslide [128] (Figure 6b). The first slope failure occurred ca. 10,000 years b.p. and involved an estimated volume of 40 million m^3. The second slope failure, with a volume of 8 million m^3, occurred ca. 7700 years b.p. [128]. Over the 2300-year gap, slope-damage-generating processes were likely activated and/or exacerbated by stress concentrations due to decreased lateral support, similar to the 1965 Hope Slide.

(**a**)　　　　　　　　　　　　　　　(**b**)
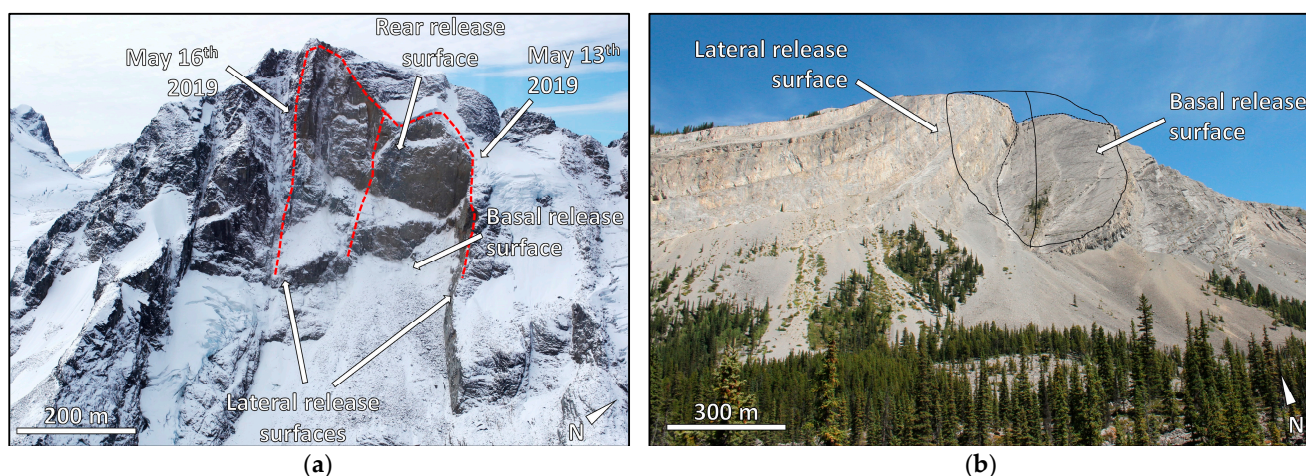
Figure 6. (**a**) Oblique view of the 2019 Joffre Peak landslide scar. The red, dashed curves outline the areas involved in the events of 13 and 16 May. It has been suggested that the failure was triggered by increased water pressure due to permafrost degradation, in combination with progressive slope damage accumulation along the basal surface. (**b**) View of the Palliser rockslide release surfaces from the deposit. The black curve shows the inferred 8 million m^3 block that detached during the most recent event, 7700 years b.p., which detached 2300 years after the initial, 40 million m^3 event.

Some preliminary observations can be made with regard to the effect of scale on multistage landslides; in particular, it should be noted that with increasing landslide volumes, a longer gap between events has often been estimated (Table 2). The correlation between the size of the events and the time gap is a subject requiring further research, including investigation of the potential role of slope damage evolution and its impacts on the long-term stability of rock slopes.

Table 2. Summary of selected multistage landslides, highlighting the potential relationship between the estimated volume and the time gap between successive events.

Multistage Landslide	Volumes Involved	Time Gap between Events
Joffre Peak [126,127]	1st event: ca. 3 million m^3 2nd event: ca. 3 million m^3	3 days
Randa rockslide [12,13]	1st event: ca. 22 million m^3 2nd event: ca. 7 million m^3	22 days
Palliser rockslide [64,128]	1st event: ca. 40 million m^3 2nd event: ca. 8 million m^3	ca. 2300 years
Hope Slide [15,16]	1st event: ca. 47 million m^3 2nd event: ca. 47 million m^3	ca. 7000 years
Elliot Creek Slide [129,130] [1]	1st event: ca. 20 million m^3 2nd event: ca. 10 million m^3	Unknown (>71 years)

[1] The age of the first event is unknown; volume of first event from unpublished data.

At smaller scales, local increases in rockfall rates can represent preparatory factors for larger slope failures. Kromer et al. [40] performed terrestrial laser scanner (TLS) monitoring to investigate the stability and evolution of a rock slope along a railroad corridor in the White Canyon (BC, Canada). In the months preceding its detachment, they noted a progressive increase in small (up to 3 m^3) rockfall activity in the area surrounding a large (2800 m^3) unstable block. They concluded that the progressive release of material from rock slopes enhances the kinematic freedom of potentially unstable blocks, ultimately promoting failure. A similar conclusion can be derived from the frame analysis of a variety of rockfall videos that are freely available online (e.g., on YouTube.com), which show increased rates of small rockfalls prior to the occurrence of larger failures (Figure 7).
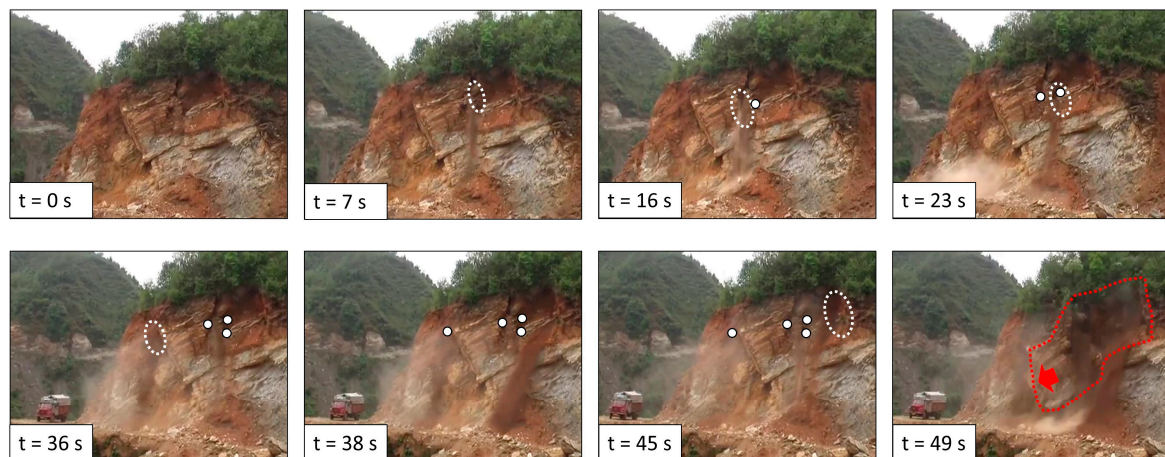
Figure 7. Frame analysis of a rockslide captured on video, showing a series of rockfalls prior to the failure, likely promoted by the excavation for the construction of the road. In each frame, the location of the identified rockfall is outlined by the white circle, and previous rockfalls are indicated by the white dots. At t = 49 s, the failure occurs (red outline and arrow). Note that in the video there is a gap of several seconds between the 23 s and 36 s frames (from https://www.youtube.com/watch?v=bWswUEp2CsE, accessed on 2 December 2022, user: Yashwant Mahar).

Based on a survey of the published literature and online media, it can be reasonably suggested that many large failures are preceded by increasing rates of material detachment. As precursory rockfalls cause a decrease in the overall stability of the slope, they can be considered to be a form of slope damage, potentially capable of controlling the detachment and, thus, the kinematics of blocks within rock slopes.

6. The Role of Rock Mass Quality and Lithology in Slope Damage and Slope Kinematics

The concept of "rock mass quality" is broadly used to describe the lithological and structural configuration of the rock mass and, in turn, the overall mechanical behavior. High-quality rock masses are generally recognized as rock masses with a relatively low degree of fracturing, high intact rock strength, and limited surface and matrix weathering and alterations. Conversely, low-quality rock masses are identified as having a higher degree of fracturing, lower intact rock strength, and more intense weathering and alterations. In the published literature, the quantification of rock mass quality using the "geological strength index" (GSI), originally introduced by Hoek et al. [131,132] to estimate rock mass strength and deformability, has become increasingly popular in practice [38,89,90,133], and the association between GSI and rock mass quality is widely accepted today. The importance of scale, however, cannot be overstated. The methods used for performing slope stability analyses (e.g., planar and wedge analysis, roto-translational sliding) and slope damage assessment must take into consideration the size of the investigated or expected slope instability; different types of landslides (e.g., structurally controlled vs. brittle-damage-

controlled vs. rock-mass-controlled and weak rock/soil-like failures) can occur in rock masses with similar GSI (and, hence, rock mass quality), depending on the size of the slope.

6.1. Effects of Low Rock Mass Quality

According to Hoek et al. [131,132], expanded upon by Cai et al. [134], depending on the scale and the quality of the rock mass, different types of behavior can be observed for rock slopes. Low-quality rock masses (as well as higher quality for bench- and slope-scale instabilities) can behave, in certain conditions, as a continuum material, due to the high degree of fracturing, small block size (compared to the size of the instability), and high fracture connectivity, (a measure of the degree of interconnection of the discontinuities within a rock mass [135]). As a result, slope damage will be largely controlled by the overall strength and deformability of the rock mass, with observed slope damage features similar to soil slopes (e.g., roto-translational failure scarps, grabens, counterscarps), accommodating large displacements prior to a slope failure. Thus, slopes formed in low quality rock masses are more affected by prolonged low-energy instability phenomena that result from the progressive slope damage accumulation, rather than episodic, high-energy instability events that affect the slopes formed by high-quality rock masses.

Various landslides have been described in the literature as displaying evidence of significant deformation and, in turn, the development of major slope damage features across the slope. Clayton et al. [70] investigated the progressive deformation of the Mitchell Creek landslide (AK, USA), which is currently active. They mapped slope damage features, such as lineaments and scarps, which were then used in combination with aerial imagery interpretation to infer the failure mechanism of the landslide. Roberti et al. [136] analyzed the geomorphic features that developed prior to the occurrence of the 2010 Mt. Meager rock avalanche (BC, Canada). They observed that several slump scarps formed at the slope surface, as a result of the slope displacement that ultimately led to the failure. Rechberger et al. [137] investigated the slow, ongoing deformation at the Marzellkamm rock slide (Austria). They mapped scarps, counterscarps, and grabens near the headscarp and across the landslide area. Slope damage mapping was then used in combination with monitoring data to reconstruct the evolution and progressive failure mechanism of the landslide. Slope damage that develops within the transition zone in large, bi- and multiplanar landslides is also controlled by rock mass quality, in view of the complex combination of dilation, shear, tensile, and brittle damage that occurs therein.

Low-quality rock masses are also more prone to developing landslide-induced shear zones. In particular, the basal release surfaces of landslides in thinly foliated rock masses (characterized by a prominent anisotropy parallel to the foliation) are often characterized by damage zones similar to those observed near fault zones (e.g., [138]). The Downie Slide (BC, Canada) involves successions of marbles, quartzites, and schists. Based on borehole logging and inclinometer monitoring data, it was observed that the displacement occurs along two distinct shear zones, referred to as the upper and lower shear zones (USZ and LSZ [28,139]). Both the USZ and LSZ are significantly more damaged, sheared, and altered than the rock mass that constitutes the rest of the landslide; the LSZ, along which most of the 300 m displacement of the landslide occurred, reaches a thickness up to 60 m at the base of the transition zone [28] (Figure 8). At the Vajont Slide, Italy, a 40–50 m thick shear zone was observed and interpreted as the base of the paleo-landslide of Mt. Toc [140] that reactivated in 1963, after the impoundment of the Vajont Reservoir.
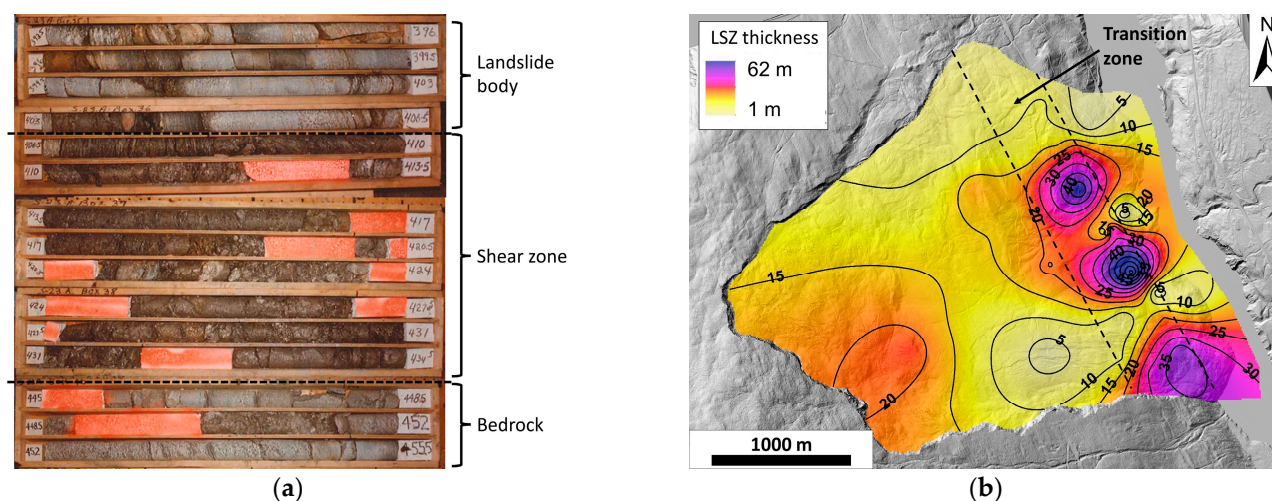
Figure 8. (**a**) Photographs of a section of the core (between depths of 120 m and 138 m) drilled through the Downie Slide. Note the sheared, altered rock and lower recovery observed within the LSZ, compared to the rock above (i.e., within the landslide body) and below the shear zone (i.e., within the stable bedrock). (**b**) Map of LSZ thickness of the Downie Slide. Note the increase—up to more than 60 m—within the transition zone between active and passive blocks in the lower slope (modified from [28]).

The presence of a slope-parallel foliation or bedding is not necessarily associated with shear zones that are tens of meters thick. The Åknes Slide (Norway) is an active, slowly moving rockslide that is displacing along a sliding surface parallel to the foliation. There, a damaged shear zone has formed with a thickness up to 40–50 cm [141]. In this case, however, the cumulative displacement is up to 30 m, based on the width of the open fracture at the rear of the landslide [141]. This is about one-tenth of the displacement estimated for the Downie Slide, suggesting that the amount of shearing along the sliding surface plays a role in defining the thickness of the shear zone. The scale of the instability and the undulation of the incipient rupture surface may also be important in controlling the formation and the thickness of basal shear zones. Larger landslides with a deeper rupture surface may promote the formation of a thicker damage zone, due to the vertical stresses that increase with depth. The LSZ of the Downie Slide, for instance, is located at a depth of up to 250 m, compared to the 65 m of the Åknes Slide. Landslides and slope instabilities that develop at the outcrop or bench scale, on the other hand, are less likely to develop thick shear zones, due to the lower stresses available along the basal surface.

6.2. Effects of High Rock Mass Quality

High-quality rock masses, with poorly interconnected fracture networks, will predominantly develop brittle slope damage features, likely displaying very limited displacement prior to a slope failure (e.g., [17,142]). The progressive accumulation of slope damage (i.e., through brittle and/or subcritical fracture propagation) in high-quality rock masses characterized by non-persistent discontinuities results in an increase in fracture connectivity [82], which can cause a generalized decrease in rock mass properties (if distributed in a large volume) and/or in the formation of new, previously unavailable rupture surfaces, potentially capable of changing the kinematics of rock slopes. An increase in rock mass connectivity can also affect the hydrogeological properties (e.g., permeability, porosity) of a rock mass, enhancing rainfall and snowmelt infiltration and percolation, further contributing to instabilities due to increased water pressure. However, an increase in permeability and porosity may also lead, in drier conditions, to a reduction in pore water pressure, due to a decrease in the water table elevation. In other words, a complex interaction may exist between slope damage development and pore water pressure, making the analysis of this correlation and relationship particularly challenging.

The 1991 Randa rockslides occurred within a massive, crystalline rock mass with a discontinuity network characterized by low discontinuity persistence and connectivity. The events did not involve the instantaneous displacement of a large block but, rather, the progressive detachment of a series of rockfalls over a period of several hours [13,17]. This prolonged activity, which allowed the event to be captured on camera, represents a peculiarity of the Randa rockslides, and it was interpreted as the effect of progressive development of brittle damage due to stress concentration and strength degradation [17]. The localized increase in fracture connectivity also likely promoted the gradual detachment of blocks from the rock slope. Leith [14] also investigated the role of long-term stress accumulation, due to far-field tectonic stresses and geomorphic valley evolution, on the landslide occurrence. In particular, the high-quality rock mass allowed for the formation of a high, sub-vertical "knob" at the intersection between two alpine valleys, from which the Randa rockslide detached. The high stress concentration, together with the high rock mass quality, was a critical factor in determining the evolution of the landslide.

The 2014 San Leo landslide [142] also displayed features typical of a brittle-damage-controlled event—particularly the observation of rough, fresh surfaces across the scar, and the absence of significant deformations prior to the landslide (Figure 9). Donati et al. [55] and Spreafico et al. [143] employed a combination of remote sensing and numerical modelling analyses to investigate the event. They highlighted the critical role played by intact rock fracturing and discontinuity propagation not only in the evolution of the landslide, but also in the slope kinematics, with damage allowing the occurrence of an oblique toppling failure that would not have been feasible otherwise [55].

6.3. Resistant-Over-Recessive (ROR) Stratigraphy and Slope Damage

The San Leo landslide occurred in a litho-geomorphological environment that can be described as resistant-over-recessive (ROR, [144]), in which a strong material (namely, limestones and sandstones forming the San Leo plateau) stratigraphically overlies a softer material (i.e., clay shales) [142]. In such cases, the behavior and deformability of the soft, basal material can significantly impact the deformation behavior (damage) and stability of the more competent layer. Indeed, Spreafico et al. [143] suggested that the accumulation of brittle damage and, ultimately, the failure of the San Leo landslide were partly driven by weathering and softening in the underlying clay-rich materials. The northern Apennines in Italy display several sites with similar geomorphological and lithological characteristics, such as the San Marino Plateau (San Marino), the Pietra di Bismantova Plateau [145], and the Sasso Simone and Simoncello. ROR succession can also occur in significantly different lithologies. The Civita di Bagnoregio Plateau (Italy) consists exclusively of pyroclastic rocks (Figure 10), with thinly stratified tuffs in the lower part, and a massive ignimbrite in the upper part of the plateau, overlying a clay deposit [146]. In this slope, the softening, swelling, and deformations within the basal clayey material cause damage to develop in the overlying volcanic rocks (Figure 10a,b), with the characteristics of the slope damage features varying significantly across the plateau [59]. The stratified tuffs, characterized by a low GSI, display a ubiquitous, rock-mass-controlled accumulation of slope damage that results in roto-translational, soil-like failures. Conversely, within the massive ignimbrite, characterized by high GSI values, brittle slope damage features develop (i.e., fracturing in intact material and propagation of sub-vertical cooling cracks; Figure 10c).
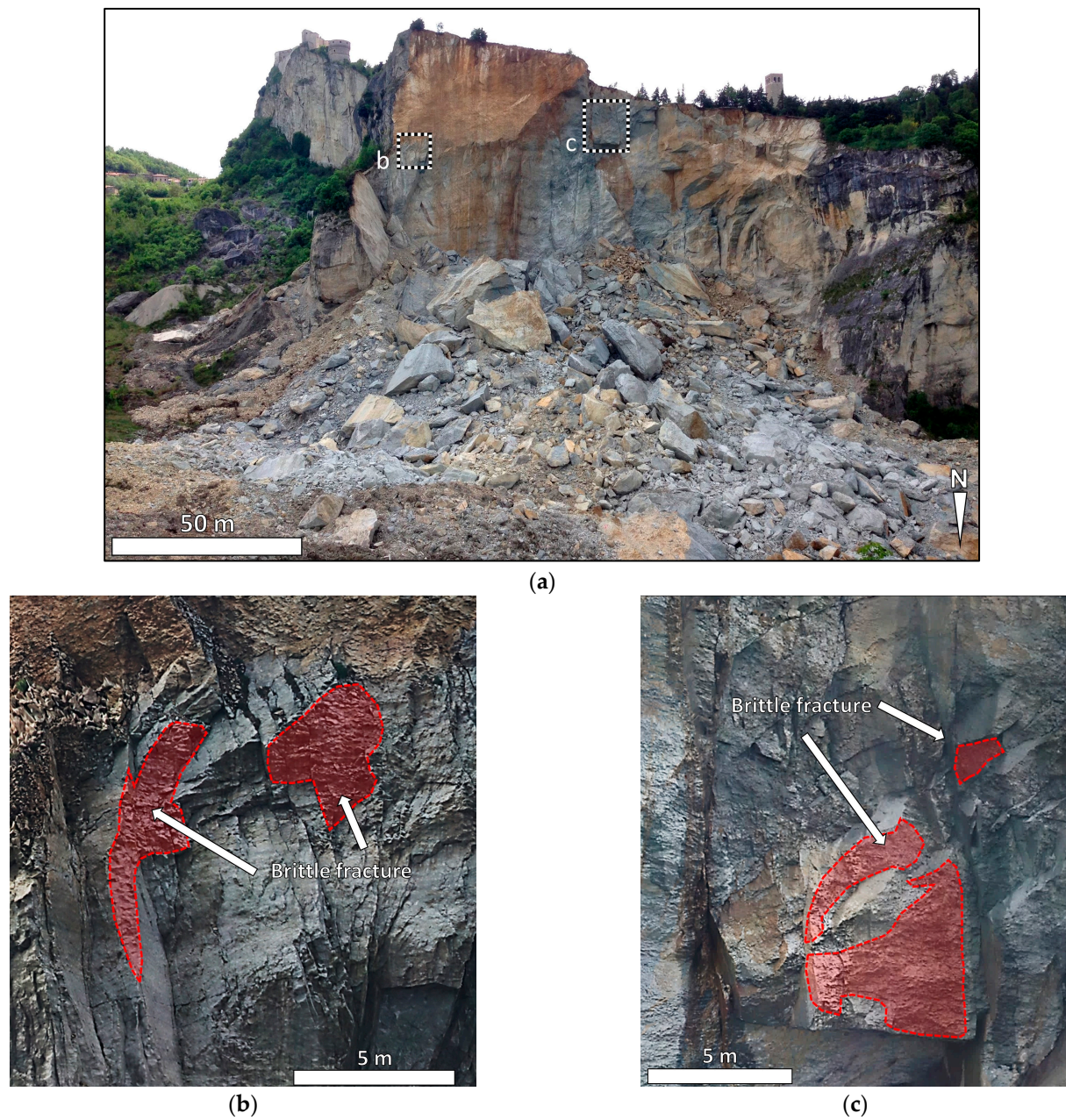
Figure 9. Slope damage at the 2014 San Leo landslide site: (**a**) View of the landslide scar. The failure was driven by progressive accumulation of brittle damage and fracture propagation along the incipient rear release surface. The locations of the photographs in b and c are indicated by the black and white squares. (**b**,**c**) High-resolution photographs showing areas where brittle slope damage occurred. The failure of out-of-plane rock bridges is evidenced by rough, fresh surfaces (modified from [55]).

Figure 10. Rock mass and slope damage at Civita di Bagnoregio: (**a**) View of the volcanic plateau. Note the varying behavior of the materials that characterize the area, particularly the landslide developing in the clayey deposit. White, dashed lines mark the boundaries between the different materials. (**b**) Slope damage features (dashed red curves) affecting the stratified tuff, inducing a decrease in the overall rock mass quality that, in turn, affects the failure and deformation behavior of the slope. (**c**) Brittle damage, in the form of a fracture propagation from the tip of a cooling fracture, in the massive ignimbrite.

7. The Characterization of Slope Damage: Methods, Challenges, and Considerations

The previous chapters showed how, depending on the scale of the instability and the structural and geomorphic conditions of the slope, the type, distribution, and role of slope damage can vary significantly.

Slope damage can be an effect of the instability's evolution and a kinematic requirement for the landslide displacement or slope deformation to progress. At the outcrop scale, brittle slope damage along the boundaries of a potentially unstable block can allow the detachment of rockfalls. At the bench scale, localized brittle damage and discontinuity dilation and shearing can allow the displacement on non-daylighting wedges. At the slope scale, the accumulation of slope damage within the transition zone of a biplanar landslide is produced by stress concentration caused by the deformation in the upper, active block, while at the same time being required for the displacement of the landslide. These examples show that slope damage is critical in controlling both the long-term stability of rock slopes and their kinematics. Moreover, the fact that slope damage development is often controlled by episodic, seasonal, and time-dependent processes highlights the importance of considering the time factor in slope stability analysis, where damage is deemed to have an impact.

Despite the key role played by slope damage in controlling the evolution of rock slopes, no framework has yet been developed that can be effectively used to clearly assess,

describe, and communicate information on the type, characteristics, and potential effects of the slope damage affecting rock slopes. In fact, the characterization and description of slope damage varies significantly not only across different disciplines (e.g., engineering geology, geomorphology), but also across different communities and research groups within the same field.

7.1. Methods and Approaches for the Characterization of Slope Damage

In geomorphology, the focus in the analysis of slope damage is directed towards surface features, such as fractures, graben, scarps, bulges, ridges, and others. Engineering geomorphological mapping approaches have been developed to systematically map and classify deformation features observed within unstable slopes and landslide deposits [10,75,147,148]. In the fields of engineering geology and rock mechanics, there is a need to investigate slope damage not only at the surface, but also deep within rock slopes. The concepts of internal and surface (or external) slope damage have recently been introduced [149]. Internal slope damage features develop deep within the slope, and they can include intact rock fracturing, as well as discontinuity and rock mass dilation. Internal slope damage can be investigated directly, through logging of high-quality drilled rock cores (e.g., [150]), and indirectly, through geophysical methods (e.g., [12]).

The distinction of extensile, compressive, and shear damage has also been introduced to describe features that develop under different stress conditions [149]. Rock mass bulging and shearing are typical features that characterize compressive slope damage, whereas discontinuity dilation and tensile rock fracturing represent features of extensile slope damage. Spatially, internal and surface slope damage can also be qualitatively distinguished in focused (e.g., dilation or propagation of a single fracture) or distributed damage (e.g., dilation and shearing of large volumes of rock mass) [80].

Over the past decade, the analysis of slope damage, particularly at the slope surface, has greatly benefited from the use of remote sensing datasets. The advantage of remotely sensed data—in particular those collected from airborne platforms—compared to traditional field techniques lies in their capability of investigating large areas, regardless of site accessibility or vegetation cover. This characteristic allows for the systematic mapping of slope damage features [28,151].

Remote sensing methods also allow for a series of repeated surveys to be undertaken, enabling temporal investigation of surface damage. Donati et al. [29] exploited a series of airborne laser scanning (ALS) datasets collected at the 10-Mile Slide (British Columbia, Canada) to develop maps of slope damage feature intensity (SD_{21}), as well as its changes with time across the landslide area. The concept of "intensity" was originally introduced in discrete fracture network engineering to quantify the degree of fracturing of rock masses [152]. Specifically, fracture intensity was defined as the ratio between the cumulative number of fractures over the core or scanline length (P_{10}), the cumulative fracture trace length over the window area (P_{21}), or the cumulative fracture area over the rock mass volume (P_{32}). A similar approach has been employed by Tuckey and Stead [153] to quantify the intensity of intact rock bridges (RB_{21}) within rock masses using digital photogrammetry data.

Damage characterization in numerical models has also received attention over the past decade. Lupogo et al. [154] employed a blast damage intensity approach to quantify brittle damage behind the face of open-pit mines excavated using explosives. Hamdi et al. [155] used a similar approach to quantify the degree of fracturing occurring in a rock specimen subjected to uniaxial compressive tests in 2D and 3D numerical models. Havaej et al. [92] used an approach referred to as an "ellipsoid of damage" to describe the location and extent of the volume of rock mass within a slope, in which brittle damage was simulated in numerical models.

7.2. A Kinematics-Based Slope Damage Characterization

In slope characterization and rock slope stability analyses, limited consideration is currently given to the impacts of slope damage on kinematics. Based on the slope damage features and mechanisms described in this paper, as well as on the experience gained by the authors in the field mapping, characterization, and numerical modelling of rock slope instabilities at various scales, it is suggested that four different types of rock slope damage can be distinguished, namely, type 1, type 2, type 3, and type 4, based on spatial distribution, time of formation, and the effects produced on the slope kinematics.

Type 1 slope damage develops at the boundaries of blocks or landslide bodies that are completely or almost completely separated from the remaining part of the slope. It includes mechanical processes such as the failure of in-plane or out-of-plane rock bridges and the shearing of asperities, along discrete rupture surfaces. Type 1 slope damage can potentially control the stability of the landslide, as it causes a decrease in the shear or tensile strength of the rupture surfaces; however, its impacts are limited from the viewpoint of slope kinematics, as no significant changes in failure or deformation mechanisms occur. The events depicted in Figure 2 are examples of outcrop-scale instabilities potentially controlled by type 1 slope damage. However, instabilities at the bench and slope scales can also be controlled by type 1 slope damage, e.g., the Val Pola landslide (Figure 3a) and Palliser rockslide (Figure 6b).

Type 2 slope damage comprises coalescing features that can provide new, previously unavailable rupture surfaces, potentially allowing the detachment of otherwise kinematically stable blocks. The localized intact rock fracturing (i.e., brittle damage) at the base of a non-daylighting block is an example of type 2 slope damage. The progressive fracture propagation and coalescence that occurred at the back of the 2014 San Leo landslide (Figure 9), causing the formation of a persistent rupture surface, is also an example of type 2 slope damage. Type 2 slope damage can control both the stability of the landslide and the potential deformation or failure mechanism, allowing the displacement of blocks that were previously constrained or irremovable. The development of type 2 slope damage is spatially limited to incipient or developing rupture surfaces and does not necessarily entail (or produce) internal deformation within the landslide, which can separate from the rock slope as an undeformed, rigid body. An exception is represented by slope damage accumulating at the hinge (or root) zone of a flexural toppling instability, which can result in the formation of a persistent rupture surface (e.g., [156,157]) but develops only after a significant slope deformation has occurred. Type 2 slope damage generally involves a significant amount of intact rock fracturing and, thus, requires sufficiently high stress magnitudes, such as in multi-bench-scale instabilities.

Compared to slope damage of type 1 and 2, type 3 slope damage develops within the landslide body and causes internal deformation that is kinematically required for the displacement and failure of the landslide. Rock mass and discontinuity dilation and intact rock fracturing occurring within the transition zones of bi- and multiplanar landslides are examples of type 3 slope damage. The Vajont Slide (Figure 3b) and the Downie Slide (Figure 8), in view of their bi- and multiplanar configuration, are examples of landslides controlled by type 3 slope damage.

Type 4 slope damage includes features that develop after the detachment and during the displacement of the landslide. Therefore, type 4 slope damage produces no significant effect on the pre-failure stability of the slope or the kinematics of the slope, but it play have an important role in landslide runout distance and the post-failure behavior of the landslide body and deposit. The fragmentation and comminution of the landslide body and/or the debris are examples of type 4 slope damage, which can be referred to as "post failure landslide damage". Figure 11a shows frames extracted from an online video showing type 4 damage features that develop during the failure of landslides. Features such as ridges, scarps, and ripples that can be observed in the landslide deposit (e.g., [10,148,158]) can also be considered examples of type 4 slope damage. The surface slope damage observed at the

Downie Slide and described in [28] developed during the post-glacial displacement of the landslide, and can therefore also be considered an example of type 4 slope damage.
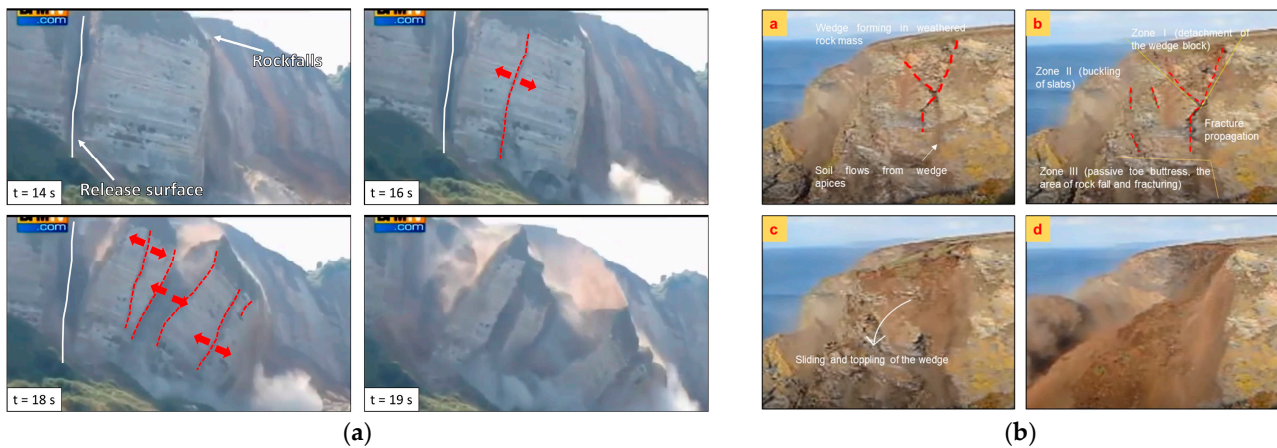

(**a**)

(**b**)

Figure 11. Examples of type 4 slope damage: (**a**) Frames extracted from an online video of the toppling failure of a sea cliff in France (from https://www.youtube.com/watch?v=gvSe27Ht-NY, accessed on 2 December 2022). The white line shows the existing release surface at the rear of the unstable block. Red, dashed lines mark fractures that opened during the displacement of the landslide, which did not affect the detachment or the kinematics of the landslide. At t = 16 s, note the rockfalls preceding the detachment of the block, enhancing its kinematic freedom. (**b**) Frame video analysis showing the development of slope damage during the displacement of a landslide that affected the Hell's Mouth cliff (Cornwall, UK, from [159]).

Table 3 summarizes the various types of slope damage, outlining the potential effects on slope kinematics and stability.

Table 3. Summary of the proposed subdivision of slope damage type, based on the effects on slope stability and kinematics.
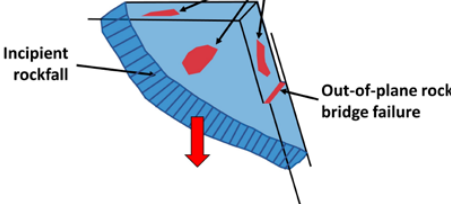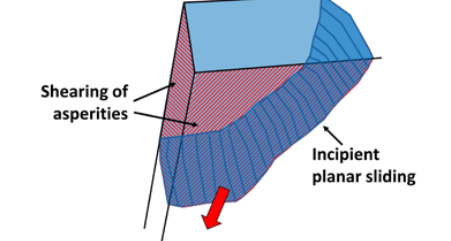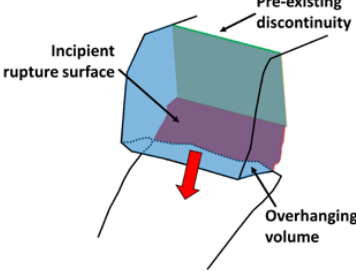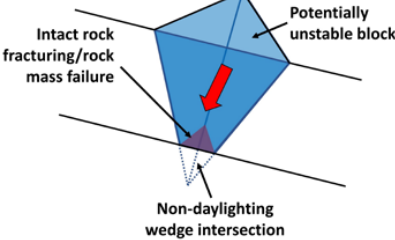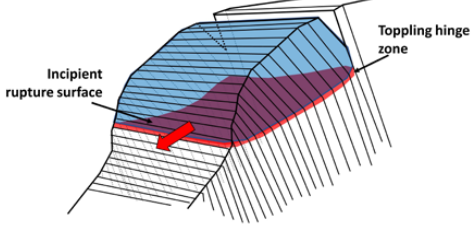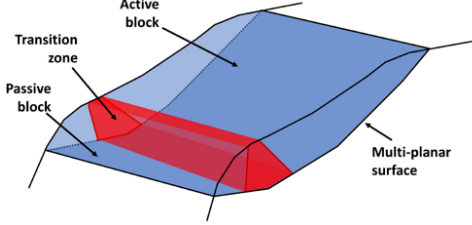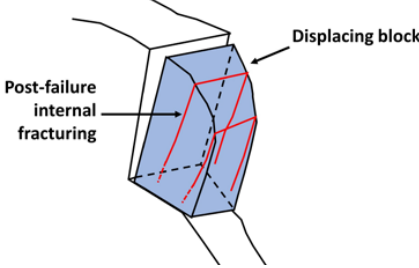
Slope Damage Type	Conceptual Examples	Effects on Slope Stability and Kinematics
Type 1	Incipient rockfall (overhanging) Sliding block (non-overhanging) 	Slope damage accumulation promotes instability by reducing shear and tensile strength along rupture surface through shearing of asperities and brittle fracturing of in-plane and out-of-plane rock bridges. Limited effect on failure or deformation kinematics.

Table 3. *Cont.*

Slope Damage Type	Conceptual Examples	Effects on Slope Stability and Kinematics
Type 2	Fracture propagation forming release surface Non-daylighting wedge Hinge (root) zone in flexural toppling	Slope damage accumulation causes instability through the formation of a new, fully persistent rupture surface that provides kinematic freedom to the landslide, thereby controlling the failure kinematics.
Type 3	Active–passive transition zone damage	Slope damage formation and accumulation within the landslide body, allowing for the deformation of the slope and the displacement of the landslide.
Type 4	Post-failure cracking	Features develop within and at the surface of the landslide body, after and as a result of its deformation, without any effect on the pre-failure behavior of the slope.

8. Final Remarks

A wide range of factors can potentially control the stability of rock slopes. One of these factors is slope damage; however, the analysis of the development and accumulation of damage within rock slopes is often overlooked, particularly in rock slope analysis and characterization. Slope damage is generally considered only as an effect or a byproduct of the slope deformation. It is suggested that the accumulation of slope damage is often a critical factor in controlling not only the stability of rock slopes, but also their kinematics. Damage accumulation within the transition zone in bi- or multiplanar landslides, and localized brittle damage that can allow the displacement of non-daylighting wedges, are just two examples of the critical control that slope damage can have over rock slope kinematics. Moreover, the fact that the development of slope damage is often controlled by episodic, seasonal, and time-dependent processes highlights the importance of considering time as a factor in slope stability analysis where damage is suspected to have an impact.

Despite the important role played by slope damage in controlling the stability and kinematics of rock slopes at all scales and with time, guidelines or frameworks to comprehensively and quantitatively assess slope damage have yet to be developed. This paper aims to highlight the importance of considering slope damage by providing insight into the effects of damage on slope kinematics, along with an initial, preliminary framework for the qualitative description of slope damage features based on its effect on slope kinematics.

It should be emphasized that rock slopes and landslides, particularly those affected by geological structures, should be considered as objects in which the deformation and failure mechanism is controlled by (a) three-dimensional structural and lithological features, (b) time-dependent slope damage formation and accumulation, and (c) the progressive geomorphological evolution of the slope. Of these, the lithological, structural, and geomorphic characteristics can now be easily reconstructed using traditional and remote sensing methods. In contrast, inferring the amount of slope damage that has accumulated within a slope over time represents a significant challenge, and yet it is often critical in correctly assessing the long-term stability of a slope. Thus, additional efforts should be made towards the analysis of slope damage, as well as the development of innovative methods combining field, geophysical, remote sensing, and numerical modelling analyses to provide an integrated slope damage model. This would undoubtedly benefit from a multidisciplinary approach, with an overriding objective being the development of a comprehensive framework for slope damage characterization and classification. Importantly, the results of our research on an integrated characterization–monitoring–numerical modelling approach can provide insight on the state and evolution of slope damage, both qualitatively (i.e., type of slope damage features) and quantitatively (e.g., intensity and spatial distribution). The numerical modelling component proved to be a very effective tool for investigating the effects of a range of events (e.g., earthquakes, groundwater fluctuations, slope steepening due to erosion or excavation) on the development of slope damage and, more generally, on slope stability. The use of a characterization–monitoring–numerical modelling approach (e.g., [51,143,159,160]) within a multidisciplinary methodology would enhance our understanding of time-dependent slope processes and, ultimately, contribute to improving the safety and livelihood of communities affected by landslide risk.

Author Contributions: Conceptualization, D.D., D.S. and L.B.; visualization, D.D.; writing—original draft preparation, D.D.; writing—review and editing, D.S. and L.B.; supervision, D.D., D.S. and L.B.; funding acquisition, D.S. and L.B. All authors have read and agreed to the published version of the manuscript.

Conflicts of Interest: The authors declare no conflict of interest.

References

1. Garcia-Delgado, H.; Petley, D.N.; Bermúdez, M.A.; Sepúlveda, S.A. Fatal Landslides in Colombia (from Historical Times to 2020) and Their Socio-Economic Impacts. *Landslides* **2022**, *19*, 1689–1716. [CrossRef]
2. Petley, D. Global Patterns of Loss of Life from Landslides. *Geology* **2012**, *40*, 927–930. [CrossRef]
3. Brideau, M.-A.; Stead, D. Evaluating Kinematic Controls on Planar Translational Slope Failure Mechanisms Using Three-Dimensional Distinct Element Modelling. *Geotech. Geol. Eng.* **2012**, *30*, 991–1011. [CrossRef]
4. Badger, T.C. Fracturing within Anticlines and Its Kinematic Control on Slope Stability. *Environ. Eng. Geosci.* **2002**, *8*, 19–33. [CrossRef]
5. Zhuang, Y.; Xing, A.; Jiang, Y.; Sun, Q.; Yan, J.; Zhang, Y. Typhoon, Rainfall and Trees Jointly Cause Landslides in Coastal Regions. *Eng. Geol.* **2022**, *298*, 106561. [CrossRef]
6. Marc, O.; Behling, R.; Andermann, C.; Turowski, J.M.; Illien, L.; Roessner, S.; Hovius, N. Long-Term Erosion of the Nepal Himalayas by Bedrock Landsliding: The Role of Monsoons, Earthquakes and Giant Landslides. *Earth Surf. Dyn.* **2019**, *7*, 107–128. [CrossRef]
7. Dellow, S.; Massey, C.; Cox, S.; Archibald, G.; Begg, J.; Bruce, Z.; Carey, J.; Davidson, J.; Pasqua, F.D.; Glassey, P.; et al. Landslides Caused by the Mw7.8 Kaikōura Earthquake and the Immediate Response. *Bull. N. Z. Soc. Earthq. Eng.* **2017**, *50*, 106–116. [CrossRef]
8. Barlow, J.; Barisin, I.; Rosser, N.; Petley, D.; Densmore, A.; Wright, T. Seismically-Induced Mass Movements and Volumetric Fluxes Resulting from the 2010 Mw=7.2 Earthquake in the Sierra Cucapah, Mexico. *Geomorphology* **2015**, *230*, 138–145. [CrossRef]
9. Jian, W.; Xu, Q.; Yang, H.; Wang, F. Mechanism and Failure Process of Qianjiangping Landslide in the Three Gorges Reservoir, China. *Environ. Earth Sci.* **2014**, *72*, 2999–3013. [CrossRef]
10. Wolter, A.; Stead, D.; Ward, B.C.; Clague, J.J.; Ghirotti, M. Engineering Geomorphological Characterisation of the Vajont Slide, Italy, and a New Interpretation of the Chronology and Evolution of the Landslide. *Landslides* **2016**, *13*, 1067–1081. [CrossRef]
11. Massey, C.; Pasqua, F.D.; Holden, C.; Kaiser, A.; Richards, L.; Wartman, J.; McSaveney, M.J.; Archibald, G.; Yetton, M.; Janku, L. Rock Slope Response to Strong Earthquake Shaking. *Landslides* **2017**, *14*, 249–268. [CrossRef]
12. Willenberg, H.; Loew, S.; Eberhardt, E.; Evans, K.F.; Spillmann, T.; Heincke, B.; Maurer, H.; Green, A.G. Internal Structure and Deformation of an Unstable Crystalline Rock Mass above Randa (Switzerland): Part I—Internal Structure from Integrated Geological and Geophysical Investigations. *Eng. Geol.* **2008**, *101*, 1–14. [CrossRef]
13. Sartori, M.; Baillifard, F.; Jaboyedoff, M.; Rouiller, J.-D. Kinematics of the 1991 Randa Rockslides (Valais, Switzerland). *Nat. Hazards Earth Syst. Sci.* **2003**, *3*, 423–433. [CrossRef]
14. Leith, K.J. Stress Development and Geomechanical Controls on the Geomorphic Evolution of Alpine Valleys. Ph.D. Thesis, ETH Zurich, Zurich, Switzerland, 2012.
15. Mathews, W.H.; McTaggart, K.C. The Hope Landslide, British Columbia. *Proc. Geol. Assoc. Can.* **1969**, *20*, 65–75.
16. Donati, D.; Stead, D.; Brideau, M.A.; Ghirotti, M. Using Pre-Failure and Post-Failure Remote Sensing Data to Constrain the Three-Dimensional Numerical Model of a Large Rock Slope Failure. *Landslides* **2021**, *18*, 827–847. [CrossRef]
17. Eberhardt, E.; Stead, D.; Coggan, J.S. Numerical Analysis of Initiation and Progressive Failure in Natural Rock Slopes—The 1991 Randa Rockslide. *Int. J. Rock Mech. Min. Sci.* **2004**, *41*, 69–87. [CrossRef]
18. Gischig, V.; Preisig, G.; Eberhardt, E. Numerical Investigation of Seismically Induced Rock Mass Fatigue as a Mechanism Contributing to the Progressive Failure of Deep-Seated Landslides. *Rock Mech. Rock Eng.* **2016**, *49*, 2457–2478. [CrossRef]
19. Kachanov, L.M. *Introduction to Continuum Damage Mechanics*; Springer: Dordrecht, The Netherlands, 1986; Volume 10, ISBN 978-90-481-8296-1.
20. Paventi, M. Rock Mass Characteristics and Damage at the Birchtree Mine. Ph.D. Thesis, McGill University, Montreal, QC, Canada, 1996.
21. Stead, D.; Coggan, J.S.; Eberhardt, E. Realistic Simulation of Rock Slope Failure Mechanisms: The Need to Incorporate Principles of Fracture Mechanics. *Int. J. Rock Mech. Min. Sci.* **2004**, *41*, 466. [CrossRef]
22. Brideau, M.-A.; Yan, M.; Stead, D. The Role of Tectonic Damage and Brittle Rock Fracture in the Development of Large Rock Slope Failures. *Geomorphology* **2009**, *103*, 30–49. [CrossRef]
23. Stead, D.; Elmo, D.; Yan, M.; Coggan, J.S. Modeling Brittle Fracture in Rock Slopes: Experience Gained and Lessons Learned. In Proceedings of the International Symposium on Rock Slope Stability in Open Pit Mining and Civil Engineering, Perth, Australian, 12–14 September 2007.
24. Collins, B.D.; Jibson, R.W. Assessment of Existing and Potential Landslide Hazards Resulting from the April 25, 2015 Gorkha, Nepal Earthquake Sequence. In *U.S. Geological Survey Open-File Report*; Geology, Minerals, Energy, and Geophysics Science Center U.S. Geological Survey: Menlo Park, CA, USA, 2015; 50p. [CrossRef]
25. Preisig, G.; Eberhardt, E.; Smithyman, M.; Preh, A.; Bonzanigo, L. Hydromechanical Rock Mass Fatigue in Deep-Seated Landslides Accompanying Seasonal Variations in Pore Pressures. *Rock Mech. Rock Eng.* **2016**, *49*, 2333–2351. [CrossRef]
26. Paronuzzi, P.; Bolla, A. Gravity-Induced Rock Mass Damage Related to Large En Masse Rockslides: Evidence from Vajont. *Geomorphology* **2015**, *234*, 28–53. [CrossRef]
27. Havaej, M.; Wolter, A.; Stead, D. The Possible Role of Brittle Rock Fracture in the 1963 Vajont Slide, Italy. *Int. J. Rock Mech. Min. Sci.* **2015**, *78*, 319–330. [CrossRef]

28. Donati, D.; Westin, A.M.; Stead, D.; Clague, J.J.; Stewart, T.W.; Lawrence, M.S.; Marsh, J. A Reinterpretation of the Downie Slide (British Columbia, Canada) Based on Slope Damage Characterization and Subsurface Data Interpretation. *Landslides* **2021**, *18*, 1561–1583. [CrossRef]

29. Donati, D.; Stead, D.; Lato, M.; Gaib, S. Spatio-Temporal Characterization of Slope Damage: Insights from the Ten Mile Slide, British Columbia, Canada. *Landslides* **2020**, *17*, 1037–1049. [CrossRef]

30. Toshioka, T.; Tsuchida, T.; Sasahara, K. Application of GPR to Detecting and Mapping Cracks in Rock Slopes. *J. Appl. Geophys.* **1995**, *33*, 119–124. [CrossRef]

31. Hancox, G.T.; Perrin, N.D.; Dellow, G.D. Recent Studies of Historical Earthquake-Induced Landsliding, Ground Damage, and MM Intensity in New Zealand. *Bull. N. Z. Soc. Earthq. Eng.* **2002**, *35*, 59–95. [CrossRef]

32. Bonzanigo, L.; Eberhardt, E.; Loew, S. Long-Term Investigation of a Deep-Seated Creeping Landslide in Crystalline Rock. Part I. Geological and Hydromechanical Factors Controlling Campo Vallemaggia. *Can. Geotech. J.* **2007**, *44*, 1157–1180. [CrossRef]

33. Bedoui, S.E.; Guglielmi, Y.; Lebourg, T.; Pérez, J.L. Deep-Seated Failure Propagation in a Fractured Rock Slope over 10,000 Years: The La Clapière Slope, the South-Eastern French Alps. *Geomorphology* **2009**, *105*, 232–238. [CrossRef]

34. Vyazmensky, A.; Stead, D.; Elmo, D.; Moss, A. Numerical Analysis of Block Caving-Induced Instability in Large Open Pit Slopes: A Finite Element/Discrete Element Approach. *Rock Mech. Rock Eng.* **2010**, *43*, 21–39. [CrossRef]

35. Moore, J.R.; Gischig, V.; Burjanek, J.; Loew, S.; Fäh, D. Site Effects in Unstable Rock Slopes: Dynamic Behavior of the Randa Instability (Switzerland)Short Note. *Bull. Seismol. Soc. Am.* **2011**, *101*, 3110–3116. [CrossRef]

36. Cheon, D.S.; Jung, Y.B.; Park, E.S.; Song, W.K.; Jang, H.I. Evaluation of Damage Level for Rock Slopes Using Acoustic Emission Technique with Waveguides. *Eng. Geol.* **2011**, *121*, 75–88. [CrossRef]

37. Amitrano, D.; Gruber, S.; Girard, L. Evidence of Frost-Cracking Inferred from Acoustic Emissions in a High-Alpine Rock-Wall. *Earth Planet. Sci. Lett.* **2012**, *341–344*, 86–93. [CrossRef]

38. Agliardi, F.; Crosta, G.B.; Meloni, F.; Valle, C.; Rivolta, C. Structurally-Controlled Instability, Damage and Slope Failure in a Porphyry Rock Mass. *Tectonophysics* **2013**, *605*, 34–47. [CrossRef]

39. Havaej, M.; Stead, D.; Eberhardt, E.; Fisher, B.R. Characterization of Bi-Planar and Ploughing Failure Mechanisms in Footwall Slopes Using Numerical Modelling. *Eng. Geol.* **2014**, *178*, 109–120. [CrossRef]

40. Kromer, R.A.; Hutchinson, D.J.; Lato, M.J.; Gauthier, D.; Edwards, T. Identifying Rock Slope Failure Precursors Using LiDAR for Transportation Corridor Hazard Management. *Eng. Geol.* **2015**, *195*, 93–103. [CrossRef]

41. Vivas, J.; Stead, D.; Elmo, D.; Hunt, C. Simulating the Interaction between Groundwater and Brittle Failure in Open Pit Slopes. In Proceedings of the 13th International ISRM Congress, Montreal, QC, Canada, 10–13 May 2015.

42. Parker, R.N.; Hancox, G.T.; Petley, D.N.; Massey, C.I.; Densmore, A.L.; Rosser, N.J. Spatial Distributions of Earthquake-Induced Landslides and Hillslope Preconditioning in the Northwest South Island, New Zealand. *Earth Surf. Dyn.* **2015**, *3*, 501–525. [CrossRef]

43. Teza, G.; Marcato, G.; Pasuto, A.; Galgaro, A. Integration of Laser Scanning and Thermal Imaging in Monitoring Optimization and Assessment of Rockfall Hazard: A Case History in the Carnic Alps (Northeastern Italy). *Nat. Hazards* **2015**, *76*, 1535–1549. [CrossRef]

44. Bonilla-Sierra, V.; Scholtès, L.; Donzé, F.V.; Elmouttie, M. DEM Analysis of Rock Bridges and the Contribution to Rock Slope Stability in the Case of Translational Sliding Failures. *Int. J. Rock Mech. Min. Sci.* **2015**, *80*, 67–78. [CrossRef]

45. Collins, B.D.; Stock, G.M. Rockfall Triggering by Cyclic Thermal Stressing of Exfoliation Fractures. *Nat. Geosci.* **2016**, *9*, 395–400. [CrossRef]

46. Riva, F.; Agliardi, F.; Crosta, G.B.; Amitrano, D. Damage-Based Long Term Modelling of a Large Alpine Rock Slope. In *Landslides and Engineered Slopes. Experience, Theory and Practice*; CRC Press: Boca Raton, FL, USA, 2016; ISBN 978-1-315-37500-7.

47. de Vilder, S.J.; Rosser, N.J.; Brain, M.J. Forensic Analysis of Rockfall Scars. *Geomorphology* **2017**, *295*, 202–214. [CrossRef]

48. Lupogo, K. Characterization of Blast Damage in Rock Slopes: An Integrated Field-Numerical Modelling Approach. Ph. D. Thesis, Simon Fraser University, Burnaby, BC, Canada, 2017.

49. Codeglia, D.; Dixon, N.; Fowmes, G.J.; Marcato, G. Analysis of Acoustic Emission Patterns for Monitoring of Rock Slope Deformation Mechanisms. *Eng. Geol.* **2017**, *219*, 21–31. [CrossRef]

50. Danielson, J. An Investigation into the Time Dependent Deformation Behaviour of Open Pit Slopes at Gibraltar Mine. M. Sc. Thesis, Simon Fraser University, Burnaby, BC, Canada, 2018.

51. Hamdi, P.; Stead, D.; Elmo, D.; Töyrä, J. Use of an Integrated Finite/Discrete Element Method-Discrete Fracture Network Approach to Characterize Surface Subsidence Associated with Sub-Level Caving. *Int. J. Rock Mech. Min. Sci.* **2018**, *103*, 55–67. [CrossRef]

52. Riva, F.; Agliardi, F.; Amitrano, D.; Crosta, G.B. Damage-Based Time-Dependent Modeling of Paraglacial to Postglacial Progressive Failure of Large Rock Slopes. *J. Geophys. Res. Earth Surf.* **2018**, *123*, 124–141. [CrossRef]

53. Guerin, A.; Jaboyedoff, M.; Collins, B.D.; Derron, M.H.; Stock, G.M.; Matasci, B.; Boesiger, M.; Lefeuvre, C.; Podladchikov, Y.Y. Detection of Rock Bridges by Infrared Thermal Imaging and Modeling. *Sci. Rep.* **2019**, *9*, 13138. [CrossRef] [PubMed]

54. Bolla, A.; Paronuzzi, P. Numerical Investigation of the Pre-Collapse Behavior and Internal Damage of an Unstable Rock Slope. *Rock Mech. Rock Eng.* **2019**, *53*, 2279–2300. [CrossRef]

55. Donati, D.; Stead, D.; Elmo, D.; Borgatti, L. A Preliminary Investigation on the Role of Brittle Fracture in the Kinematics of the 2014 San Leo Landslide. *Geosciences* **2019**, *9*, 256. [CrossRef]

56. Donati, D.; Stead, D.; Stewart, T.W.; Marsh, J. Numerical Modelling of Slope Damage in Large, Slowly Moving Rockslides: Insights from the Downie Slide, British Columbia, Canada. *Eng. Geol.* **2020**, *273*, 105693. [CrossRef]

57. Piller, T. Characterizing the Checkerboard Creek Rock Slope Using a Combined Remote Sensing and Numerical Modelling Approach. Available online: https://summit.sfu.ca/item/35174 (accessed on 3 February 2023).

58. Paronuzzi, P.; Bolla, A. In-Depth Field Survey of a Rockslide Detachment Surface to Recognise the Occurrence of Gravity-Induced Cracking. *Eng. Geol.* **2022**, *302*, 106636. [CrossRef]

59. Donati, D.; Borgatti, L.; Stead, D.; Francioni, M.; Ghirotti, M.; Margottini, C. The Characterization of Slope Damage at the Civita Di Bagnoregio Plateau Using a Remote Sensing Approach. In *Geotechnical Engineering for the Preservation of Monuments and Historic Sites III*; CRC Press: Boca Raton, FL, USA, 2022; pp. 497–508. [CrossRef]

60. Rechberger, C.; Zangerl, C. Rock Mass Characterisation and Distinct Element Modelling of a Deep-Seated Rock Slide Influenced by Glacier Retreat. *Eng. Geol.* **2022**, *300*, 106584. [CrossRef]

61. Sharif, L.K.; Elmo, D.; Stead, D. New Approaches to Quantify Progressive Damage and Associated Dynamic Rock Mass Blockiness. *J. Rock Mech. Geotech. Eng.* **2023**, *15*, 285–295. [CrossRef]

62. Wyllie, D. *Rock Slope Engineering*, 5th ed.; CRC Press: Boca Raton, FL, USA, 2017; ISBN 978-1-4987-8627-0.

63. Stead, D.; Wolter, A. A Critical Review of Rock Slope Failure Mechanisms: The Importance of Structural Geology. *J. Struct. Geol.* **2015**, *74*, 1–23. [CrossRef]

64. Sturzenegger, M.; Stead, D. The Palliser Rockslide, Canadian Rocky Mountains: Characterization and Modeling of a Stepped Failure Surface. *Geomorphology* **2012**, *138*, 145–161. [CrossRef]

65. Brideau, M.-A.; Stead, D. Controls on Block Toppling Using a Three-Dimensional Distinct Element Approach. *Rock Mech. Rock Eng.* **2010**, *43*, 241–260. [CrossRef]

66. Corkum, A.G.; Martin, C.D. Analysis of a Rock Slide Stabilized with a Toe-Berm: A Case Study in British Columbia, Canada. *Int. J. Rock Mech. Min. Sci.* **2004**, *41*, 1109–1121. [CrossRef]

67. Wolter, A.; Havaej, M.; Zorzi, L.; Stead, D.; Clague, J.J.; Ghirotti, M.; Genevois, R. Exploration of the Kinematics of the 1963 Vajont Slide, Italy, Using a Numerical Modelling Toolbox. *Ital. J. Eng. Geol. Environ.* **2013**, 585–598. [CrossRef]

68. Kos, A.; Amann, F.; Strozzi, T.; Delaloye, R.; von Ruette, J.; Springman, S. Contemporary Glacier Retreat Triggers a Rapid Landslide Response, Great Aletsch Glacier, Switzerland. *Geophys. Res. Lett.* **2016**, *43*, 412–466, 474. [CrossRef]

69. Evans, S.G.; Clague, J.J. Recent Climatic Change and Catastrophic Geomorphic Processes in Mountain Environments. *Geomorphology* **1994**, *10*, 107–128. [CrossRef]

70. Clayton, A.; Stead, D.; Kinakin, D.; Wolter, A. Engineering Geomorphological Interpretation of the Mitchell Creek Landslide, British Columbia, Canada. *Landslides* **2017**, *14*, 1655–1675. [CrossRef]

71. McColl, S.T.; Davies, T.R.H.; McSaveney, M.J. Glacier Retreat and Rock-Slope Stability: Debunking Debuttressing. In *Delegate Papers, Geologically Active, 11th Congress of the International Association for Engineering Geology and the Environment*; CRC Press: Auckland, New Zealand, 2010; pp. 467–474.

72. Grämiger, L.M.; Moore, J.R.; Gischig, V.S.; Ivy-Ochs, S.; Loew, S. Beyond Debuttressing: Mechanics of Paraglacial Rock Slope Damage during Repeat Glacial Cycles. *J. Geophys. Res. Earth Surf.* **2017**, *122*, 1004–1036. [CrossRef]

73. Larsen, I.J.; Montgomery, D.R. Landslide Erosion Coupled to Tectonics and River Incision. *Nat. Geosci.* **2012**, *5*, 468–473. [CrossRef]

74. Mysiorek, J.; Onsel, E.; Stead, D.; Rosser, N.J. Engineering Geological Characterization of the 2014 Jure Landslide, Nepal: An Interactive Mixed-Reality Approach to Slope Characterization. In Proceedings of the Under Land and Sea. GeoStJohn 2019—72nd Canadian Geotechnical Conference, St. John's, NL, Canada, 29 September 29–2 October 2019.

75. Griffiths, J.S.; Stokes, M.; Stead, D.; Giles, D. Landscape Evolution and Engineering Geology: Results from IAEG Commission 22. *Bull. Eng. Geol. Environ.* **2012**, *71*, 605–636. [CrossRef]

76. Andriani, G.F.; Walsh, N. Rocky Coast Geomorphology and Erosional Processes: A Case Study along the Murgia Coastline South of Bari, Apulia—SE Italy. *Geomorphology* **2007**, *87*, 224–238. [CrossRef]

77. Lim, M.; Rosser, N.J.; Allison, R.J.; Petley, D.N. Erosional Processes in the Hard Rock Coastal Cliffs at Staithes, North Yorkshire. *Geomorphology* **2010**, *114*, 12–21. [CrossRef]

78. McAdoo, B.G.; Quak, M.; Gnyawali, K.R.; Adhikari, B.R.; Devkota, S.; Rajbhandari, P.L.; Sudmeier-Rieux, K. Roads and Landslides in Nepal: How Development Affects Environmental Risk. *Nat. Hazards Earth Syst. Sci.* **2018**, *18*, 3203–3210. [CrossRef]

79. Kalkani, E.C.; Piteau, D.R. Finite Element Analysis of Toppling Failure at Hell's Gate Bluffs, British Columbia. *Bull. Assoc. Eng. Geol.* **1976**, *13*, 315–327. [CrossRef]

80. Donati, D.; Stead, D.; Elmo, D.; Onsel, E. New Techniques for Characterising Damage in Rock Slopes: Implications for Engineered Slopes and Open Pit Mines. In Proceedings of the 2020 International Symposium on Slope Stability in Open Pit Mining and Civil Engineering, Perth, Australia, 12–14 May 2020; Australian Centre for Geomechanics: Crawley, Australia, 2020; pp. 129–144.

81. Rose, N.D.; Hungr, O. Forecasting Potential Rock Slope Failure in Open Pit Mines Using the Inverse-Velocity Method. *Int. J. Rock Mech. Min. Sci.* **2007**, *44*, 308–320. [CrossRef]

82. Elmo, D.; Donati, D.; Stead, D. Challenges in the Characterisation of Intact Rock Bridges in Rock Slopes. *Eng. Geol.* **2018**, *245*, 81–96. [CrossRef]

83. Kalenchuk, K.S.; Diederichs, M.S.; McKinnon, S. Characterizing Block Geometry in Jointed Rockmasses. *Int. J. Rock Mech. Min. Sci.* **2006**, *43*, 1212–1225. [CrossRef]

84. Tatone, B.S.A.; Grasselli, G. Modeling Direct Shear Tests with FEM/DEM: Investigation of Discontinuity Shear Strength Scale Effect as an Emergent Characteristic. In Proceedings of the 46th US Rock Mechanics/Geomechanics Symposium, Chicago, IL, USA, 24–27 June 2012.

85. Goodman, R.E. Block Theory and Its Application. *Géotechnique* **1995**, *45*, 383–423. [CrossRef]

86. Goodman, R.E.; Shi, G. *Block Theory and Its Application to Rock Engineering*; Hall, W.J., Ed.; Prentice-Hall: Hoboken, NJ, USA, 1985; ISBN 978-0-13-078189-5.

87. Einstein, H.H.; Veneziano, D.; Baecher, G.B.; O'Reilly, K.J. The Effect of Discontinuity Persistence on Rock Slope Stability. *Int. J. Rock Mech. Min. Sci. Geomech. Abstr.* **1983**, *20*, 227–236. [CrossRef]

88. Dershowitz, W.S.; Finnila, A.; Rogers, S.; Hamdi, P.; Moffitt, K.M. Step Path Rock Bridge Percentage for Analysis of Slope Stability. In Proceedings of the 51st US Rock Mechanics/Geomechanics Symposium 2017, San Francisco, CA, USA, 25–28 June 2017; Volume 5.

89. Brideau, M.-A.; Stead, D.; Kinakin, D.; Fecova, K. Influence of Tectonic Structures on the Hope Slide, British Columbia, Canada. *Eng. Geol.* **2005**, *80*, 242–259. [CrossRef]

90. Pedrazzini, A.; Jaboyedoff, M.; Froese, C.R.; Langenberg, C.W.; Moreno, F. Structural Analysis of Turtle Mountain: Origin and Influence of Fractures in the Development of Rock Slope Failures. *Geol. Soc. Lond. Spec. Publ.* **2011**, *351*, 163–183. [CrossRef]

91. Barton, N. The Shear Strength of Rock and Rock Joints. *Int. J. Rock Mech. Min. Sci. Geomech. Abstr.* **1976**, *13*, 255–279. [CrossRef]

92. Havaej, M.; Stead, D.; Lorig, L.; Vivas, J. Modelling Rock Bridge Failure and Brittle Fracturing In Large Open Pit Rock Slopes. In Proceedings of the 46th US Rock Mechanics/Geomechanics Symposium, Chicago, IL, USA, 24–27 June 2012.

93. Azzoni, A.; Chiesa, S.; Frassoni, A.; Govi, M. The Valpola Landslide. *Eng. Geol.* **1992**, *33*, 59–70. [CrossRef]

94. Crosta, G.B.; Chen, H.; Lee, C.F. Replay of the 1987 Val Pola Landslide, Italian Alps. *Geomorphology* **2004**, *60*, 127–146. [CrossRef]

95. Semenza, E.; Ghirotti, M. History of the 1963 Vaiont Slide: The Importance of Geological Factors. *Bull. Eng. Geol. Environ.* **2000**, *59*, 87–97. [CrossRef]

96. Kalenchuk, K.S.; Hutchinson, D.J.; Diederichs, M.S. Geomechanical Interpretation of the Downie Slide Considering Field Data and Three-Dimensional Numerical Modelling. *Landslides* **2013**, *10*, 737–756. [CrossRef]

97. Kvapil, R.; Clews, M. An Examination of the Prandtl Mechanism in Large Dimension Slope Failures. *Trans. Inst. Min. Metall. Sect. A* **1979**, *88*, A1–A5.

98. Pánek, T.; Klimeš, J. Temporal Behavior of Deep-Seated Gravitational Slope Deformations: A Review. *Earth-Sci. Rev.* **2016**, *156*, 14–38. [CrossRef]

99. Cornelius, R.R.; Scott, P.A. A Materials Failure Relation of Accelerating Creep as Empirical Description of Damage Accumulation. *Rock Mech. Rock Eng.* **1993**, *26*, 233–252. [CrossRef]

100. Chandler, H.D. Creep Modelling Using Semiempirical Deformation and Damage Equations: F.c.c. Metals. *Mater. Sci. Eng. A* **1991**, *131*, 177–185. [CrossRef]

101. Campanella, R.G.; Vaid, Y.P. Triaxial and Plane Strain Creep Rupture of an Undisturbed Clay. *Can. Geotech. J.* **1974**, *11*, 1–10. [CrossRef]

102. Chigira, M. Long-Term Gravitational Deformation of Rocks by Mass Rock Creep. *Eng. Geol.* **1992**, *32*, 157–184. [CrossRef]

103. Huang, R.Q.; Wu, L.Z.; He, Q.; Li, J.H. Stress Intensity Factor Analysis and the Stability of Overhanging Rock. *Rock Mech. Rock Eng.* **2017**, *50*, 2135–2142. [CrossRef]

104. Atkinson, B.K. Subcritical Crack Growth in Geological Materials. *J. Geophys. Res. Solid Earth* **1984**, *89*, 4077–4114. [CrossRef]

105. Kemeny, J. A Model for Non-Linear Rock Deformation under Compression Due to Sub-Critical Crack Growth. *Int. J. Rock Mech. Min. Sci. Geomech. Abstr.* **1991**, *28*, 459–467. [CrossRef]

106. Kemeny, J. Time-Dependent Drift Degradation Due to the Progressive Failure of Rock Bridges along Discontinuities. *Int. J. Rock Mech. Min. Sci.* **2005**, *42*, 35–46. [CrossRef]

107. Kemeny, J. The Time-Dependent Reduction of Sliding Cohesion Due to Rock Bridges along Discontinuities: A Fracture Mechanics Approach. *Rock Mech. Rock Eng.* **2003**, *36*, 27–38. [CrossRef]

108. Sampaleanu, C.; Stead, D.; Donati, D.; Griffiths, C.; D'Ambra, S.; LeBreton, R. Characterizing Brittle Fracture Induced Rockfall in an Open Sub-Level Retreat Excavation. In Proceedings of the 51st US Rock Mechanics/Geomechanics Symposium 2017, San Francisco, CA, USA, 25–28 June 2017.

109. Evans, S.G.; Couture, R. The 1965 Hope Slide, British Columbia; Catastrophic Failure of a Sagging Rock Slope. In Proceedings of the Geological Society of America Meeting, Denver, CO, USA, 27–30 October 2002. Paper No. 16-6.

110. Grøneng, G.; Lu, M.; Nilsen, B.; Jenssen, A.K. Modelling of Time-Dependent Behavior of the Basal Sliding Surface of the Åknes Rockslide Area in Western Norway. *Eng. Geol.* **2010**, *114*, 414–422. [CrossRef]

111. Chigira, M.; Kenzo, K. Deep-Seated Rockslide-Avalanches Preceded by Mass Rock Creep of Sedimentary Rocks in the Akaishi Mountains, Central Japan. *Eng. Geol.* **1994**, *38*, 221–230. [CrossRef]

112. Marc, O.; Meunier, P.; Hovius, N. Prediction of the Area Affected by Earthquake-Induced Landsliding Based on Seismological Parameters. *Nat. Hazards Earth Syst. Sci.* **2017**, *17*, 1159–1175. [CrossRef]

113. Azhari, A.; Ozbay, U. Investigating the Effect of Earthquakes on Open Pit Mine Slopes. *Int. J. Rock Mech. Min. Sci.* **2017**, *100*, 218–228. [CrossRef]

114. Wolter, A.; Gischig, V.; Stead, D.; Clague, J.J. Investigation of Geomorphic and Seismic Effects on the 1959 Madison Canyon, Montana, Landslide Using an Integrated Field, Engineering Geomorphology Mapping, and Numerical Modelling Approach. *Rock Mech. Rock Eng.* **2016**, *49*, 2479–2501. [CrossRef]

115. Gischig, V.S.; Eberhardt, E.; Moore, J.R.; Hungr, O. On the Seismic Response of Deep-Seated Rock Slope InstabilitiesInsights from Numerical Modeling. *Eng. Geol.* **2015**, *193*, 1–18. [CrossRef]

116. Eberhardt, E.; Bonzanigo, L.; Loew, S. Long-Term Investigation of a Deep-Seated Creeping Landslide in Crystalline Rock. Part II. Mitigation Measures and Numerical Modelling of Deep Drainage at Campo Vallemaggia. *Can. Geotech. J.* **2007**, *44*, 1181–1199. [CrossRef]

117. Matsuoka, N. Direct Observation of Frost Wedging in Alpine Bedrock. *Earth Surf. Process. Landf.* **2001**, *26*, 601–614. [CrossRef]

118. Matsuoka, N. A Model of the Rate of Frost Shattering: Application to Field Data from Japan, Svalbard and Antarctica. *Permafr. Periglac. Process.* **1991**, *2*, 271–281. [CrossRef]

119. Murton, J.B.; Peterson, R.; Ozouf, J.-C. Bedrock Failure by Ice Segregation in Cold Regions. *Science* **2006**, *314*, 1127–1129. [CrossRef]

120. Hales, T.C.; Roering, J.J. Climatic Controls on Frost Cracking and Implications for the Evolution of Bedrock Landscapes. *J. Geophys. Res. Earth Surf.* **2007**, *112*, 1–14. [CrossRef]

121. Matsuoka, N.; Sakai, H. Rockfall Activity from an Alpine Cliff during Thawing Periods. *Geomorphology* **1999**, *28*, 309–328. [CrossRef]

122. Zwissler, B.; Oommen, T.; Vitton, S. A Study of the Impacts of Freeze-Thaw on Cliff Recession at the Calvert Cliffs in Calvert County, Maryland. *Geotech. Geol. Eng.* **2014**, *32*, 1133–1148. [CrossRef]

123. Luo, X.; Jiang, N.; Fan, X.; Mei, N.; Luo, H. Effects of Freeze-Thaw on the Determination and Application of Parameters of Slope Rock Mass in Cold Regions. *Cold Reg. Sci. Technol.* **2015**, *110*, 32–37. [CrossRef]

124. Gunzburger, Y.; Merrien-Soukatchoff, V.; Guglielmi, Y. Influence of Daily Surface Temperature Fluctuations on Rock Slope Stability: Case Study of the Rochers de Valabres Slope (France). *Int. J. Rock Mech. Min. Sci.* **2005**, *42*, 331–349. [CrossRef]

125. Gischig, V.S.; Moore, J.R.; Evans, K.F.; Amann, F.; Loew, S. Thermomechanical Forcing of Deep Rock Slope Deformation: 2. the Randa Rock Slope Instability. *J. Geophys. Res. Earth Surf.* **2011**, *116*, 1–17. [CrossRef]

126. Friele, P.; Millard, T.H.; Mitchell, A.; Allstadt, K.E.; Menounos, B.; Geertsema, M.; Clague, J.J. Observations on the May 2019 Joffre Peak Landslides, British Columbia. *Landslides* **2020**, *17*, 913–930. [CrossRef] [PubMed]

127. Fullin, N.; Ghirotti, M.; Donati, D.; Stead, D. Characterising the Kinematics of the Joffre Peak Landslides Using a Combined Numerical Modeling-Remote Sensing Approach. In Proceedings of the 23rd EGU General Assembly, online, 19–30 April 2021.

128. Sturzenegger, M.; Stead, D.; Gosse, J.; Ward, B.; Froese, C. Reconstruction of the History of the Palliser Rockslide Based On36Cl Terrestrial Cosmogenic Nuclide Dating and Debris Volume Estimations. *Landslides* **2015**, *12*, 1097–1106. [CrossRef]

129. Geertsema, M.; Menounos, B.; Bullard, G.; Carrivick, J.L.; Clague, J.J.; Dai, C.; Donati, D.; Ekstrom, G.; Jackson, J.M.; Lynett, P.; et al. The 28 November 2020 Landslide, Tsunami, and Outburst Flood—A Hazard Cascade Associated With Rapid Deglaciation at Elliot Creek, British Columbia, Canada. *Geophys. Res. Lett.* **2022**, *49*, e2021GL096716. [CrossRef]

130. Donati, D.; Stead, D.; Geertsema, M.; Bendle, J.M.; Menounos, B.; Borgatti, L. Kinematic Analysis of the 2020 Elliot Creek Landslide, British Columbia, Using Remote Sensing Data. *Front. Earth Sci.* **2022**, *10*, 916069. [CrossRef]

131. Hoek, E.; Brown, E.T. The Hoek–Brown Failure Criterion and GSI—2018 Edition. *J. Rock Mech. Geotech. Eng.* **2019**, *11*, 445–463. [CrossRef]

132. Hoek, E.; Brown, E.T. Practical Estimates of Rock Mass Strength. *Int. J. Rock Mech. Min. Sci.* **1997**, *34*, 1165–1186. [CrossRef]

133. Agliardi, F.; Sapigni, M.; Crosta, G.B. Rock Mass Characterization by High-Resolution Sonic and GSI Borehole Logging. *Rock Mech. Rock Eng.* **2016**, *49*, 4303–4318. [CrossRef]

134. Cai, M.; Kaiser, P.K.; Uno, H.; Tasaka, Y.; Minami, M. Estimation of Rock Mass Deformation Modulus and Strength of Jointed Hard Rock Masses Using the GSI System. *Int. J. Rock Mech. Min. Sci.* **2004**, *41*, 3–19. [CrossRef]

135. Berkowitz, B. Analysis of Fracture Network Connectivity Using Percolation Theory. *Math. Geol.* **1995**, *27*, 467–483. [CrossRef]

136. Roberti, G.; Ward, B.; Vries, B. van W. de; Friele, P.; Perotti, L.; Clague, J.J.; Giardino, M. Precursory Slope Distress Prior to the 2010 Mount Meager Landslide, British Columbia. *Landslides* **2018**, *15*, 637–647. [CrossRef]

137. Rechberger, C.; Fey, C.; Zangerl, C. Structural Characterisation, Internal Deformation, and Kinematics of an Active Deep-Seated Rock Slide in a Valley Glacier Retreat Area. *Eng. Geol.* **2021**, *286*, 106048. [CrossRef]

138. Choi, J.H.; Edwards, P.; Ko, K.; Kim, Y.S. Definition and Classification of Fault Damage Zones: A Review and a New Methodological Approach. *Earth-Sci. Rev.* **2016**, *152*, 70–87. [CrossRef]

139. Kalenchuk, K.S.; Hutchinson, D.J.; Diederichs, M.S. Application of Spatial Prediction Techniques to Defining Three-Dimensional Landslide Shear Surface Geometry. *Landslides* **2009**, *6*, 321–333. [CrossRef]

140. Paronuzzi, P.; Bolla, A. The Prehistoric Vajont Rockslide: An Updated Geological Model. *Geomorphology* **2012**, *169–170*, 165–191. [CrossRef]

141. Ganerød, G.V.; Grøneng, G.; Rønning, J.S.; Dalsegg, E.; Elvebakk, H.; Tønnesen, J.F.; Kveldsvik, V.; Eiken, T.; Blikra, L.H.; Braathen, A. Geological Model of the Åknes Rockslide, Western Norway. *Eng. Geol.* **2008**, *102*, 1–18. [CrossRef]

142. Borgatti, L.; Guerra, C.; Nesci, O.; Romeo, R.W.; Veneri, F.; Landuzzi, A.; Benedetti, G.; Marchi, G.; Lucente, C.C. The 27 February 2014 San Leo Landslide (Northern Italy). *Landslides* **2015**, *12*, 387–394. [CrossRef]

143. Spreafico, M.C.; Cervi, F.; Francioni, M.; Stead, D.; Borgatti, L. An Investigation into the Development of Toppling at the Edge of Fractured Rock Plateaux Using a Numerical Modelling Approach. *Geomorphology* **2017**, *288*, 83–98. [CrossRef]

144. Jackson, L.E. Landslides and Landscape Evolution in the Rocky Mountains and Adjacent Foothills Area, Southwestern Alberta, Canada. In *Catastrophic Landslides*; The Geological Society of America: Boulder, CO, USA, 2002; Volume XV, pp. 325–344. [CrossRef]

145. Borgatti, L.; Tosatti, G. Slope Instability Processes Affecting the Pietra Di Bismantova Geosite (Northern Apennines, Italy). *Geoheritage* **2010**, *2*, 155–168. [CrossRef]

146. Delmonaco, G.; Margottini, C.; Puglisi, C. The Dying Town of Civita Di Bagnoregio and the Killer Landslide. In Proceedings of the Ninth International Symposium on Landslides, Rio de Janeiro, Brazil, 28 June–2 July 2004.

147. Griffiths, J.S.; Mather, A.E.; Stokes, M. Mapping Landslides at Different Scales. *Q. J. Eng. Geol. Hydrogeol.* **2015**, *48*, 29–40. [CrossRef]

148. Shea, T.; Vries, B. van W. de Structural Analysis and Analogue Modeling of the Kinematics and Dynamics of Rockslide Avalanches. *Geosphere* **2008**, *4*, 657. [CrossRef]

149. Stead, D.; Eberhardt, E. Understanding the Mechanics of Large Landslides. *Ital. J. Eng. Geol. Environ.* **2013**, *6*, 85–112. [CrossRef]

150. Chigira, M.; Hariyama, T.; Yamasaki, S. Development of Deep-Seated Gravitational Slope Deformation on a Shale Dip-Slope: Observations from High-Quality Drill Cores. *Tectonophysics* **2013**, *605*, 104–113. [CrossRef]

151. Stead, D.; Donati, D.; Wolter, A.; Sturzenegger, M. Application of Remote Sensing to the Investigation of Rock Slopes: Experience Gained and Lessons Learned. *ISPRS Int. J. Geo-Inf.* **2019**, *8*, 296. [CrossRef]

152. Dershowitz, W.; Hermanson, J.; Follin, S.; Mauldon, M. Fracture Intensity Measures in 1-D, 2-D, and 3-D at Aspo, Sweden. In Proceedings of the 4th North American Rock Mechanics Symposium, Seattle, WA, USA, 31 July–3 August 2000; pp. 849–853.

153. Tuckey, Z.; Stead, D. Improvements to Field and Remote Sensing Methods for Mapping Discontinuity Persistence and Intact Rock Bridges in Rock Slopes. *Eng. Geol.* **2016**, *208*, 136–153. [CrossRef]

154. Lupogo, K.; Tuckey, Z.; Stead, D.; Elmo, D. Blast Damage in Rock Slopes: Potential Applications of Discrete Fracture Network Engineering. In Proceedings of the 1st Conference on Discrete Fracture Network Engineering, Vancouver, BC, Canada, 19–22 October 2014. DFNE 2014-151.

155. Hamdi, P.; Stead, D.; Elmo, D. Damage Characterization during Laboratory Strength Testing: A 3D-Finite-Discrete Element Approach. *Comput. Geotech.* **2014**, *60*, 33–46. [CrossRef]

156. Alzo'ubi; Martin. Cruden A Discrete Element Damage Model for Rock Slopes. In Proceedings of the 1st Canada-US Rock Mechanics Symposium—Rock Mechanics Meeting Society's Challenges and Demands, Vancouver, BC, Canada, 27–31 May 2007; Volume 1, pp. 503–510.

157. Adhikary, D.P.; Dyskin, A.V.; Jewell, R.J.; Stewart, D.P. A Study of the Mechanism of Flexural Toppling Failure of Rock Slopes. *Rock Mech. Rock Eng.* **1997**, *30*, 75–93. [CrossRef]

158. Longchamp, C.; Abellan, A.; Jaboyedoff, M.; Manzella, I. 3-D Models and Structural Analysis of Rock Avalanches: The Study of the Deformation Process to Better Understand the Propagation Mechanism. *Earth Surf. Dyn.* **2016**, *4*, 743–755. [CrossRef]

159. He, L.; Coggan, J.; Stead, D.; Francioni, M.; Eyre, M. Modelling Discontinuity Control on the Development of Hell's Mouth Landslide. *Landslides* **2021**, *19*, 277–295. [CrossRef]

160. Tuckey, Z. An Integrated Field Mapping-Numerical Modelling Approach to Characterising Discontinuity Persistence and Intact Rock Bridges in Large Open Pit Slopes. Master's. Thesis, Queen's University, Kingston, ON, Canada, 2012.